

Final Report

# Women's Cardiovascular Risk from PM Exposure: A Laboratory-based Toxicology Study Using a Sensitive Animal Model

California Air Resources Board Contract Number 16RD005

Submitted 03/31/2020

Principal Investigators: Michael T. Kleinman and Ulrike  
Luderer

Submitted by

Michael Kleinman, Ulrike Luderer, David A. Herman, Rebecca Johnson  
Arechavala

## Disclaimer

*The statements and conclusions in this report are those of the investigators and not necessarily those of the California Air Resources Board. The mention of commercial products, their source, or their use in connection with material reported herein is not to be construed as actual or implied endorsement of such products.*

## Contents

Title Page.....	i
Disclaimer.....	ii
Contents.....	iii
List of Figures .....	vi
List of Tables .....	vii
Abbreviations.....	viii
Executive Summary.....	1
Introduction .....	3
Objective .....	3
Rationale .....	3
Background .....	3
PM air pollution and cardiovascular disease .....	3
<i>Association between ovarian function and cardiovascular disease</i> .....	4
<i>PM air pollution and ovarian function</i> .....	5
Materials and Methods.....	6
Animal Model.....	6
Exposure System .....	6
Exposure Monitoring .....	7
<i>Size-resolved Particle Number and Mass Concentrations</i> .....	7
Sample Collection .....	7
<i>Weekly Collection Media Preparation</i> .....	7
<i>Post-Loading Filter Storage</i> .....	8
<i>Weekly Post-Sampling Media Storage Procedures</i> .....	8
Electrocardiographic (ECG) Measurement and Analysis .....	8
<i>ECG Implantation</i> .....	8
<i>ECG Analysis</i> .....	9
<i>Heart Rate Variability</i> .....	10
Reproductive Function Analyses.....	11
<i>Estrous Cycling</i> .....	11
<i>Ovarian Follicle Analysis</i> .....	11
<i>Immunohistochemistry</i> .....	11
<i>Surgery and Hormone Replacement</i> .....	12

Echocardiogram Analysis .....	12
Cardiomyocyte Analysis .....	13
Arterial Histology .....	13
Statistics .....	13
<i>Gravimetric and OC/EC Carbon Analysis</i> .....	13
<i>ECG measurements</i> .....	13
<i>HRV analysis</i> .....	13
<i>Echocardiography</i> .....	13
<i>Lesion characterization and Inflammatory Response</i> .....	13
<i>Cardiomyocyte Contractility</i> .....	14
Results and Discussion .....	15
Comparison of Exposure-related Effects on Cardiopulmonary Physiology in Male and Female ApoE <sup>-/-</sup> Mice .....	15
<i>Particle Concentrations</i> .....	15
<i>Electrocardiography: Rate-Associated Endpoints</i> .....	15
<i>Electrocardiography: Ventricular-Associated Endpoints</i> .....	18
<i>Heart Rate Variability</i> .....	19
<i>Blood Pressure</i> .....	21
<i>Cardiopulmonary Function Measurements</i> .....	22
Effects of CAPs Exposure on Ovariectomized and Intact ApoE <sup>-/-</sup> Mice .....	24
<i>Exposure Data</i> .....	24
<i>Effects of CAPs Exposure on Ovaries in Female ApoE<sup>-/-</sup> Mice</i> .....	24
<i>Electrocardiography: Rate-Related Endpoints</i> .....	28
<i>Electrocardiography: Ventricular-Related Endpoints</i> .....	30
<i>Heart Rate Variability</i> .....	31
<i>Blood Pressure</i> .....	33
<i>Cardiac Function Measurements</i> .....	34
<i>Echocardiogram Analysis</i> .....	35
<i>Cardiomyocytes</i> .....	36
<i>Plaque Formation in Arteries of Sham and OVAX Mice</i> .....	37
Does 17 $\beta$ Estradiol (E2) Rescue Adverse Cardiovascular Effects Caused by Ovariectomy and PM Exposure? .....	38
<i>Heart Rate and Heart Rate Variability</i> .....	38
<i>Blood Pressure</i> .....	43

Limitations of this study.....	44
Summary and Conclusions.....	45
References .....	48

## List of Figures

Figure 1. Schematic diagram of the particle concentrator/exposure system .....	7
Figure 2. Idealized schematic of a typical ECG waveform.....	9
Figure 3. Sex-dependent responses in heart rate-related electrocardiographic wave form parameters. ....	17
Figure 4. Sex-dependent responses in ventricular-function-related electrocardiographic wave form parameters ....	18
Figure 5. Sex-dependent responses in heart rate variability.....	20
Figure 6. Sex-dependent changes from baseline systolic and diastolic blood pressures (Mean $\pm$ SE; n=5/group). ....	22
Figure 7. Sex-related differences in cardiopulmonary function measurements (Mean $\pm$ SE; n=5/group) .....	23
Figure 8. Primordial and primary follicle numbers per ovary. ....	25
Figure 9. Healthy and atretic secondary and antral follicles. ....	25
Figure 10. Ki67-positive granulosa cells in primordial and primary follicles.....	26
Figure 11. Caspase-3-positive granulosa cells in secondary and antral follicles.....	26
Figure 12 Percentage of follicles with granulosa cells that stained positively for gH2AX .....	27
Figure 13. Rate-related ECG endpoints: OVX vs SHAM.....	29
Figure 14. Ventricular-related ECG endpoints: OVX vs. SHAM. ....	30
Figure 15. Time-domain parameters of heart rate variability (HRV).....	31
Figure 16. Frequency-domain parameters.....	32
Figure 17. CAPs exposure decreased systolic blood pressure compared to controls in SHAM animals only but not in OVX mice.....	33
Figure 18 CAPs exposure did not alter $dp/dt$ or the rate-pressure product (RPP) in the OVX treated mice, however, CAPs-exposed intact animals exhibited decreases in both measurements compared to control animals. ....	34
Figure 19. CAPs exposure increased left ventricular (LV) myocardial mass and wall thickness in both OVX and intact animals compared to controls, suggestive of LV hypertrophy.....	35
Figure 20 Cardiomyocyte contractility parameters: OVX vs. SHAM. ....	36
Figure 21 Arterial sections representing Air-exposed and PM2.5-exposed mice which had received sham surgeries (SHAM) or ovariectomy surgery (OVAX).....	37
Figure 22 Heart rate changes as an effect of CAPs exposure. ....	39
Figure 23 Total heart rate variability represented as standard deviation of NN-intervals.....	40
Figure 24 Root mean squared of successive differences as affected by CAPs exposure and hormone treatment. ....	41
Figure 25 Ratio of low to high frequency (LF/HF) heart rate variability. ....	42
Figure 26 Systolic and diastolic blood pressure in mice exposed to Concentrated Ambient PM2.5 or purified Air. ....	43

## List of Tables

<i>Table 1. Concentrations Averaged Over Exposure Period.....</i>	<i>15</i>
<i>Table 2. Average and standard error of HR, SDNN and RMSSD of pooled change from baseline during the final 5 weeks of the exposure (weeks 7-11 from Figure 5). ....</i>	<i>21</i>
<i>Table 3. Concentrations Averaged Over Exposure Period.....</i>	<i>24</i>
<i>Table 4. Measurements of Arterial Plaque (n=5/group).....</i>	<i>37</i>
<i>Table 5 Number and Exposure of Mice for Blood Pressure Measurements.....</i>	<i>43</i>
<i>Table 6 Summary of Responses in Male and Female apoE<sup>-/-</sup> Mice Exposed to Concentrated Ambient Particles.....</i>	<i>45</i>

## Abbreviations

ApoE	apolipoprotein E
BP	blood pressure
CAAQS	California Ambient Air Quality Standards
CAPs	concentrated ambient particles
E2	17 $\beta$ -estradiol
ECG	electrocardiogram
gH2AX or $\gamma$ -H2AX	phosphorylated histone 2AX
HF	high frequency (a measurement of HRV)
HR	heart rate
HRT	hormone replacement therapy
HRV	heart rate variability
LDL	low-density lipoprotein
LF	low frequency (a measurement of HRV)
LV	left ventricle
NAAQS	National Ambient Air Quality Standards
OVAX or OVX	ovariectomized
PAH	polycyclic aromatic hydrocarbon
PM	particulate matter
PM <sub>2.5</sub>	particulate matter with an aerodynamic diameter less than 2.5 $\mu$ m
RMSSD	root mean squared of successive differences of N-N intervals
SDNN	standard deviation of N-N intervals
SH	spontaneously hypertensive
UFP	ultrafine particle
VACES	Versatile Aerosol Concentration Enrichment System

## Executive Summary

The goal of this study was to provide experimental evidence to elucidate the epidemiological finding that older women may be more susceptible than men to the cardiovascular effects associated with particulate matter (PM) exposure, especially to PM with an aerodynamic diameter less than 2.5  $\mu\text{m}$  ( $\text{PM}_{2.5}$ ). Epidemiological evidence has indicated that  $\text{PM}_{2.5}$  exposure could exacerbate cardiovascular disease severity and progression, that impaired ovarian function is associated with cardiovascular disease, and that post-menopausal women could represent a pollution-susceptible population that was inadequately studied.

The overarching hypothesis for this study was that  $\text{PM}_{2.5}$  exposure would perturb ovarian function, impair cardiovascular function in both males and females, and that the interaction of these effects would amplify the adverse cardiovascular effects of  $\text{PM}_{2.5}$  exposure in females, compared to males.

This project examined exposure-related effects in genetically modified mice in which the apoE gene was knocked out (apoE<sup>-/-</sup>). These mice were exposed to  $\text{PM}_{2.5}$  concentrated ambient particles (CAPs) 5 hours per day, 4 days per week for 12 weeks. When comparing male and female mice, there were significant sex and exposure-related differences in electrocardiographic (ECG) waveforms, blood pressure, heart rate and heart rate variability (HRV). HRV measures after exposure to  $\text{PM}_{2.5}$  CAPs generally decreased over time; females showed a greater negative HRV response to CAPs exposure than did males, highlighting sex-differences in cardiovascular effects of PM inhalation. On the other hand, male animals appeared to be more susceptible to atrial conduction anomalies as indicated by a large P-R interval elongation compared to air controls, which was not seen in the females. Chronic exposure to CAPs also produced marked changes in ventricular conduction rates. Exposed male mice experienced shorter ventricular depolarization/repolarization cycles compared to air-exposed controls while no exposure effect was seen in the female animals. There were profound effects of  $\text{PM}_{2.5}$  CAPs exposure on ovarian function, which was consistent with effects previously documented after in vivo exposure of rodents and in vitro incubation of cultured mouse ovarian follicles and neonatal ovaries with known components of PM and diesel exhaust, notably polycyclic aromatic hydrocarbons (PAHs).

Arterial plaques from mice that had been ovariectomized, or underwent a sham surgery, were analyzed for total area, the area of the artery lumen, and the percent occlusion of the artery expressed as the ratio of the area of the wall to the area of the lumen. The largest and most developed plaques are seen in the SHAM-operated group exposed to CAPs. The mean plaque size was significantly greater than that of the Air-exposed SHAM ( $p \leq 0.001$ ). A two-way ANOVA showed that there was a significant effect of exposure ( $p = 0.01$ ), a significant effect of OVAX ( $p = 0.02$ ) and a significant interaction between the CAPs exposure and the OVAX surgery ( $p = 0.01$ ). Exposure to  $\text{PM}_{2.5}$  CAPs had a direct effect on the ovaries, decreasing primary and primordial follicle numbers, resulting in about a 50% depletion of the ovarian reserve. Numbers of growing secondary follicles were also decreased. Follicle depletion was not associated with accelerated recruitment of primordial follicles into the growing pool, thus exposure-related decreased ovarian reserve that could lead to premature ovarian failure was most likely due to direct destruction of primordial follicles, which could increase the risk for cardiovascular disease in women. Thus, our data support the hypothesis that exposure to  $\text{PM}_{2.5}$  may increase risk for cardiovascular disease in women by accelerating the onset of ovarian senescence by direct destruction of primordial ovarian cells.

Further analysis of the female mice showed that PM<sub>2.5</sub> CAPs exposure induced increased left-ventricular (LV) mass and wall thickness, which are markers of hypertrophy. This finding has not been previously demonstrated under controlled conditions, to our knowledge, although there is epidemiological evidence that LV function is sub-clinically impaired in individuals chronically exposed to ambient PM<sub>2.5</sub>.

We examined whether some of the adverse effects seen in the ovariectomized mice could be rescued with hormone replacement (HRT). Female mice underwent ovariectomy or a sham ovariectomy (SHAM) procedure, and half of the ovariectomized (OVAX) mice were treated with injected pellets containing a time-release dose of 17 $\beta$ -estradiol (E2) or with a placebo pellet. Although the HRT treatment induced toxicity that became manifest 5 weeks into the exposures, the results from the first 5 weeks of study suggest that E2 treatment reduced the adverse PM-related effects noted in our first two experiments and thus provide some support for our hypothesis that ovarian toxicity, which could lead to early menopause, is an important, and previously little investigated air pollution health effect.

Our findings to date support the hypothesis that PM<sub>2.5</sub> exposure can impair ovarian function by depleting ovarian follicles which can lead to ovarian failure. We also demonstrated that HRV changes, which are indicators of shifts in the autonomic nervous system's influence on cardiac function, are induced in both males and females, but are more pronounced in females. And, our results also showed that 12-week PM<sub>2.5</sub> CAPs exposures are associated, in female mice, with remodeling of the left ventricular tissue of the heart which is an adverse change that could predict an increased risk of heart failure. However, further research is needed to continue to elucidate the mechanisms of why older females are more susceptible to adverse health effects from air pollution.

## Introduction

### Objective

The objective of this study is to provide experimental evidence to elucidate the epidemiological finding that older women may be more susceptible than men to some of the cardiovascular effects associated with particulate matter exposure. The results would provide information for consideration in the process of evaluating the adequacy of air quality standards to better protect women's health. The present study investigated the toxicity of inhaled PM<sub>2.5</sub> in females compared to males using a rodent model of cardiovascular disease. To further examine the mechanisms of PM toxicity in females, the present study also investigated responses in female mice that underwent removal of their ovaries (ovariectomy) and also looked at whether hormone replacement would be protective in the ovariectomized mice.

### Rationale

Epidemiological studies suggest that post-menopausal women have a greater relative risk of cardiovascular mortality than pre-menopausal women or men. Yet animal studies designed to shed light on the mechanism of toxicity for particulate matter have mostly been conducted using male animals. However, studies that have focused on women's health have reported an increased risk of mortality from exposure to air pollution compared to studies with combined populations of men and women. Evidence from the scientific literature shows that: (1) PM<sub>2.5</sub> exposure exacerbates cardiovascular disease severity and progression, and (2) impaired ovarian function is associated with cardiovascular disease.

### Background

PM air pollution is categorized based on the aerodynamic diameter of the particles, with those less than 10 µm in diameter designated as PM<sub>10</sub> (or coarse particles), those less than 2.5 µm designated as PM<sub>2.5</sub> (or fine particles), and those less than 0.1 µm designated as ultrafine particles (UFP). It is important to note that, by definition, PM<sub>2.5</sub> includes UFP as a component of the overall particle size distribution. Residents of California have been exposed historically to high ambient concentrations of PM, and motor vehicle traffic is a major cause of PM<sub>2.5</sub> air pollution in the state. Air quality in California has been greatly improved over the past two decades, but National Ambient Air Quality Standards (NAAQS) and California Ambient Air Quality Standards (CAAQS) continue to be exceeded, at times. Some air districts nationwide, including California's San Joaquin Valley and the South Coast Air Basin, have nonattainment areas for PM<sub>2.5</sub> air standards as currently listed by the U.S. EPA (updated 2019 - [https://www3.epa.gov/airquality/greenbook/knca.html#PM-2.5.2012.LA-South\\_Coast](https://www3.epa.gov/airquality/greenbook/knca.html#PM-2.5.2012.LA-South_Coast)).

#### *PM air pollution and cardiovascular disease*

Long-term exposures to PM<sub>2.5</sub> have been associated with increased cardiovascular mortality in general and with death from ischemic heart disease, dysrhythmias, heart failure, and cardiac arrest in a large study of participants from many US cities (Pope et al. 2004). Another multi-city study found that long-term PM<sub>2.5</sub> exposure was associated with increased incidence of nonfatal cardiovascular events and of deaths from cardiovascular diseases in postmenopausal women (Miller et al. 2007). The latter study and

several others provided evidence that the adverse cardiovascular effects of PM may be greater in women than in men.

Accumulating evidence from epidemiological and experimental studies suggests that exposure to PM increases the risk for cardiovascular disease by increasing inflammation, accelerating atherosclerosis, and decreasing cardiac autonomic function (Lewtas 2007; Pope et al. 2004). Another emerging theme from these studies is that smaller particles are associated with greater cardiovascular risk (risk from UFP > PM<sub>2.5</sub> > PM<sub>10</sub>). The observations that human atherosclerotic lesions contain polycyclic aromatic hydrocarbon (PAH)-DNA adducts and evidence of oxidative DNA damage have led to the proposal that oxidative stress, mitochondrial dysfunction, and DNA damage may be within the mechanistic pathway by which PM exposure promotes atherosclerosis (Lewtas 2007; Xia et al. 2007). Data from animal studies support these observations in humans. Apolipoprotein E (apoE) null mice exposed to PM<sub>2.5</sub> and UFP exhibited systemic oxidative stress and developed larger atherosclerotic aortic lesions than mice exposed to filtered air or PM<sub>2.5</sub> (Araujo et al. 2008). In addition, exposure to PM<sub>2.5</sub> led to increased risk of insulin resistance and diabetes mellitus, a well-established risk factor for atherosclerosis, in mice fed a high fat diet (Sun et al. 2009). Exposure to diesel exhaust, which is rich in fine particles and PAHs, altered cardiac expression of hypertension-related genes in normal rats, including down-regulation of mitochondrial genes and oxidative stress response genes (Gottipolu et al. 2009). Exposure of cultured endothelial cells, airway epithelial cells, and macrophages to PM increased generation of reactive oxygen species (ROS), decreased mitochondrial membrane potential, decreased mitochondrial calcium retention capacity, and initiated apoptosis (Kamdar et al. 2008; Li et al. 2006; Upadhyay et al. 2003; Xia et al. 2004). Mitochondrial damage plays a role in the development of cardiovascular disease as a result of exposure to tobacco smoke, which is rich in PM (Yang et al. 2007).

#### *Association between ovarian function and cardiovascular disease*

Natural and surgical menopause are well-established risk factors for cardiovascular disease in women, evidenced by the rapid progression of atherosclerotic lesions following the cessation of ovarian function (Dubey et al. 2005; Shuster et al. 2008). Studies in monkeys have shown that the progression of atherosclerosis after ovariectomy may be related to increased oxidation of low density lipoprotein (LDL), increased sympathetic arousal, and activation of the renin-angiotensin system (Kaplan et al. 1996). In fact, in LDL receptor null mice that had been ovariectomized or had chemically induced ovarian failure, estrogen replacement dramatically decreased the size of high-fat-diet-induced atherosclerotic lesions (Bourassa et al. 1996; Mayer et al. 2005). Ovariectomy of spontaneously hypertensive (SH) rats increased aortic superoxide generation, increased aortic vasoconstriction in response to angiotensin II, and increased angiotensin type 1 (AT1) receptor expression; these effects were reversed by estradiol replacement or AT1 receptor antagonism (Wassmann et al. 2001). Estradiol upregulated expression of mitochondrial and extracellular superoxide dismutase and decreased superoxide production in cultured rat vascular smooth muscle cells (Strehlow et al. 2003). SH rats had fewer large antral follicles at puberty, prior to the onset of hypertension (Pinilla et al. 2009), and hypertensive renin-overexpressing (mRen2)27 rats had lower numbers of antral follicles than control rats (de Gooyer et al. 2004). Infusion of angiotensin II in normal Sprague Dawley rats decreased numbers of ovarian antral follicles (de Gooyer et al. 2004). Rats of the (mRen2)27 strain also had increased myocardial oxidative damage and fibrosis compared to controls, both of which were reversed by inhibition of renin and by AT1 receptor blockade (Whaley-Connell et al. 2008). Thus, increased renin and angiotensin II in hypertensive animals may

decrease the number of estrogen-producing antral follicles, leading to decreased vascular antioxidant capacity.

*PM air pollution and ovarian function*

Inhalation of polluted air may affect the reproductive system. Exposure to air pollution has been associated with sperm abnormalities in men (Rubes et al. 2005; Rubes et al. 2007; Selevan et al. 2000), and these effects were proposed to be due to PAHs present on PM in polluted air (Rubes et al. 2005; Rubes et al. 2007). However, there are no studies evaluating the effects of air pollution on fertility or ovarian function in women and few animal studies examining the effects of air pollution on female reproduction. Two studies in which female mice were exposed to highly polluted urban air or filtered air as adults (Mohallem et al. 2005) or during development and continuing to adulthood (Veras et al. 2009) found evidence for decreased fertility and increased incidence of irregular estrous cycles with exposure to polluted air. The results discussed herein will begin to fill this data gap with a detailed analysis of the effects of exposure to PM<sub>2.5</sub> air pollution on ovarian follicle numbers, apoptosis, oxidative stress, and serum estradiol concentrations.

## Materials and Methods

### Animal Model

All experiments were conducted using 12-week-old genetically modified mice in which the apoE gene was knocked out (apoE<sup>-/-</sup>). Female and male apoE<sup>-/-</sup> littermates (Jackson Labs) were exposed to PM<sub>2.5</sub> concentrated ambient particles (CAPs) 5 hours per day, 4 days per week for 12 weeks. Control mice were exposed to purified (filtered) air under conditions identical to the animals that were exposed to CAPs. Tissues and plasma were collected from all mice following exposures. Between exposures, mice were housed in our vivarium, which is approved by the Association for Assessment and Accreditation of Laboratory Animal Care (AAALAC), and received water and food, ad libitum. The procedures used in this study were approved by the UC Irvine Institutional Animal Care and Use Committee.

### Exposure System

Mice were exposed to CAPs using a Versatile Aerosol Concentration Enrichment System (VACES) (S. Kim et al. 2001a; S. Kim et al. 2001b; Kleinman et al. 2007) coupled with custom-designed exposure chambers (Oldham et al. 2004). Female (n=32) and male (n=32) mice were conditioned to the exposure system in purified air at least one week before beginning CAPs exposures. Before conditioning, 12 male and 12 female mice were randomly selected from the group to be surgically implanted with telemetry devices. After conditioning, baseline averages of heart rate and measures of blood pressure and heart rate variability (HRV) were recorded for the implanted animals, and baseline blood pressure (BP) was acquired for all the mice using a non-invasive tail cuff method. Males and females were paired based on systolic blood pressure; pairs were rank-ordered with respect to BP and members of the pairs were randomized to exposed and control groups (n=16 per group). For exposures to CAPs, 16 male and 16 female mice were placed into sealed, compartmentalized exposure chambers connected to the outlet of the VACES system. Temperature was monitored continuously during the exposures and held to 75 ± 5°F. Animals were observed throughout the exposure period for signs of distress. The second and third experiments only included female mice. In experiment 2, 64 mice were randomized into 2 groups. One group was assigned to be ovariectomized (OVAX) and the second groups received a sham surgery, which mimicked the surgery preliminary to the ovariectomy but the ovaries were left intact (SHAM). ECG implantations and exposures were conducted using the same numbers and durations as for the first experiment. In the hormone replacement therapy (HRT) experiment 3, there were 6 experimental groups: (1) sham surgery, air-exposed; (2) sham surgery, CAPs-exposed; (3) OVAX mice with placebo pellet, air-exposed; (4) OVAX mice with placebo pellet, CAPs-exposed; (5) OVAX mice with E2 pellet, air-exposed; and (6) OVAX mice with E2 pellet, CAPs-exposed.

Ambient air is drawn from an elevated stack (~8 m above ground) into the VACES (Figure 1). The air stream is saturated with water vapor in a humidifier, which is a 10 L aluminum vessel half-filled with water and maintained at 38°C. The residence time in the humidifier is about 3 seconds. Doubly de-mineralized water (18.1 MΩ) is used in the humidifier. The humidified air is thus saturated with water vapor and warmed up to about 30°C (Seongheon Kim et al. 2001). The air exiting the humidifier enters a condenser, a stainless-steel pipe that is surrounded by a mixture of water and diethylene glycol, which is continuously circulated by means of a chiller. The temperature of the cooling mixture in the condenser is -3 ± 0.5°C and checked using a digital thermometer. The actual temperature of the air stream in the condenser is 20–21°C (Seongheon Kim et al. 2001). Due to the sharp drop in temperature (about 10°C)

the air in the condenser becomes strongly supersaturated. The supersaturation causes water vapor to condense onto particles as small as 20 nm in size, which rapidly grow to 2.5-3  $\mu\text{m}$  water droplets. These droplets are subsequently concentrated by a virtual impactor and exit via the minor air flow. After leaving the virtual impactor, the water content of the aerosol is reduced to near-ambient levels using silica-gel diffusion dryers (3062, TSI, Shoreview, MN, USA), returning the size distribution of the concentrated aerosol particles to nearly its original distribution.

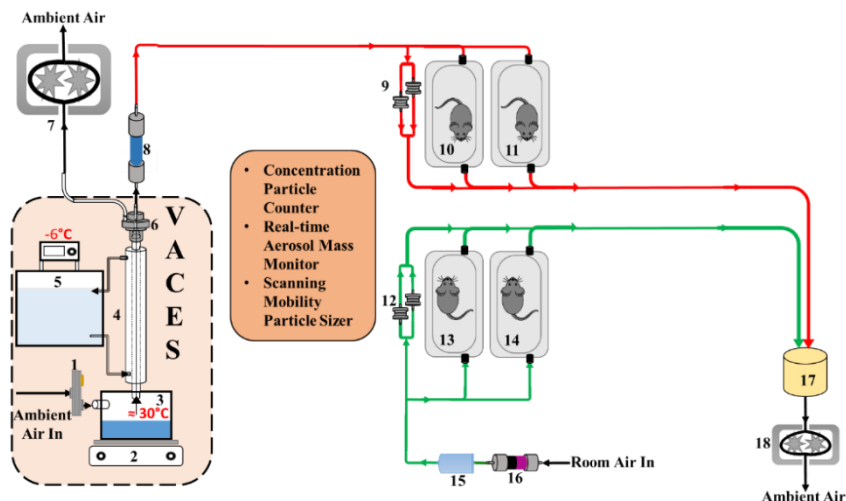


Figure 1. Schematic diagram of the particle concentrator/exposure system

1)  $\text{PM}_{2.5}$  Slit Impactor, 2) Hot plate, 3) Saturating bath ( $\approx 30^\circ\text{C}$ ), 4) Condensation tube, 5) Chiller ( $\approx -6^\circ\text{C}$ ), 6) Virtual impactor, 7) Major flow exhaust pump, 8) Diffusion dryers, 9)  $\text{PM}_{2.5}$  Teflon and quartz membrane filters, 10)  $\text{PM}_{2.5}$  Male Mice, 11)  $\text{PM}_{2.5}$  Female Mice, 12) Filtered Air Teflon and quartz membrane filters, 13) Filtered Air Male Mice, 14) Filtered Air Female Mice, 15) HEPA filter, 16) Potassium permanganate-impregnated alumina beads followed by activated carbon, 17) Exhaust dampening chamber, 18) Minor flow exhaust pump

## Exposure Monitoring

### Size-resolved Particle Number and Mass Concentrations

A TSI Scanning Mobility Particle Sizer (SMPS, Shoreview, MN, USA) was used to measure the size distribution of  $\text{PM}_{2.5}$  over the size range of 20 nm up to about 1  $\mu\text{m}$ . An optical particle counter was used to measure particle mass concentrations in the size range of 0.5  $\mu\text{m}$  to 2.5  $\mu\text{m}$  (note that particles smaller than 0.5  $\mu\text{m}$  represent a very small contribution to total  $\text{PM}_{2.5}$  mass). In addition to monitoring particle mass, a TSI condensation particle counter (Model 3022) was run in parallel to measure total particle number concentrations. A TSI DustTrak optical mass monitor (Model 8520) provided integrated  $\text{PM}_{2.5}$  mass concentrations.

## Sample Collection

### Weekly Collection Media Preparation

- Quartz Filter for organic carbon and elemental carbon (OC/EC) Analysis  
Quartz filters were baked at  $550^\circ\text{C}$  in a benchtop purge oven for 18 hours prior to use.
- Polytetrafluoroethylene (PTFE) filters for Trace Metal Analysis

PTFE filters were weighed three times before the weekly sampling using an automatic microbalance (Cahn 29, ThermoFisher, Waltham, MA, USA) after allowing at least 24 hours of equilibration in a controlled environment with temperature of 22-24°C and a relative humidity of 40-45%.

#### *Post-Loading Filter Storage*

- Quartz Filter for OC/EC Analysis

Quartz filters were immediately removed from their holders and transferred to aluminum foil-lined, parafilm-wrapped, filter cassettes and stored at -20 °C until analysis.

- PTFE Filter for Trace Metal Analysis

PTFE filters were weighed three times after the weekly sampling using an automatic microbalance (Cahn 29, ThermoFisher, Waltham, MA, USA) after allowing at least 24 hours of equilibration in a controlled environment with temperature of 22-24°C and relative humidity of 40-45%.

#### *Weekly Post-Sampling Media Storage Procedures*

- Quartz Filter:

Following sampling, the quartz filter samples were stored in aluminum foil-lined, parafilm-wrapped, filter cassettes for OC/EC analyses.

- PTFE Filter:

The loaded PTFE filter samples were removed from the sampling units, placed into parafilm-wrapped storage cassettes, and stored for trace metal analysis. The mass concentrations of aerosol particles were determined by the net filter weight gained after sampling.

## Electrocardiographic (ECG) Measurement and Analysis

### *ECG Implantation*

The iox2<sup>®</sup> (EMKA Technologies S.A.S., Falls Church, VA, USA) telemetry system is designed to detect and collect biopotential data (e.g. ECG tracings), temperature, and physical activity in mice. The devices were implanted in 5 mice from each exposure group using aseptic technique. Isoflurane was administered via inhalation to anesthetize the mice. A ~1 cm midline abdominal incision was made, and the contents of the abdomen were exposed using a retractor. The body of the telemetry device was placed on top of the intestines. A 14-gauge needle was passed through the abdominal wall lateral to the cranial aspect of the incision, going from the outside into the abdominal cavity. The negative lead was passed through the needle and out of the abdomen. The needle was withdrawn, leaving the lead externalized. Once externalized, the leads were placed in a modified Lead II configuration using hemostats to bluntly separate the connective tissue between the chest and the dermis to set the lead in the final position. Prior to implantation, the lead was stripped, leaving at least 1 cm of the wire exposed, and was secured by suturing the muscle tissue up over the lead using 4-0 non-absorbable suture. These steps were repeated for the positive lead. The device body was secured in place by incorporating the suture rib of the device into the abdominal closure using non-absorbable sutures. The skin incision was closed using skin staples. After surgery, the animal was placed into a warm environment and the breathing air supplemented with additional oxygen. Animal recovery was monitored until it was fully awake. Analgesia with buprenorphine (0.01-0.05 mg/kg body weight subcutaneously every 12 hours for three

days) was provided to all animals post-surgery. Enrofloxacin (Baytril) at a dose of 3 mg/kg body weight was administered via subcutaneous injection for 7 days.

### ECG Analysis

The ecgAUTO® (EMKA Technologies S.A.S., Falls Church, VA, USA) system was used to analyze biopotentials, body core temperature, and activity telemetry signals from each implanted animal. ECG waveforms were stored on a dedicated computer in data files for subsequent analysis. Analysis of the ECG waveform (Figure 2) was used to extract heart rate, incidence of abnormal heart beats (arrhythmias), waveform abnormalities, and measures of heart rate variability (HRV). HRV is the magnitude of variance explained (time-domain) in the heart's rhythm across different spectra (frequency-domain) of periodic oscillations in heart rate. Portions of these spectra reflect different autonomic influences on heart rate. The high frequency (HF) band (0.15-0.40 Hz) of the heart period power spectrum has been used to estimate cardiac vagal control (Liao et al. 1996). Decreased cardiac vagal activity in humans is associated with an increased risk of coronary atherosclerosis (Hayano et al. 1991). Heart period oscillations at lower frequencies (LF, 0.04-0.15 Hz) are less well understood. They may represent mixed sympathetic-parasympathetic and thermoregulatory influences (Fleisher et al. 1996; Lossius et al.) We examined ECG waveforms for evidence of exposure-related changes.

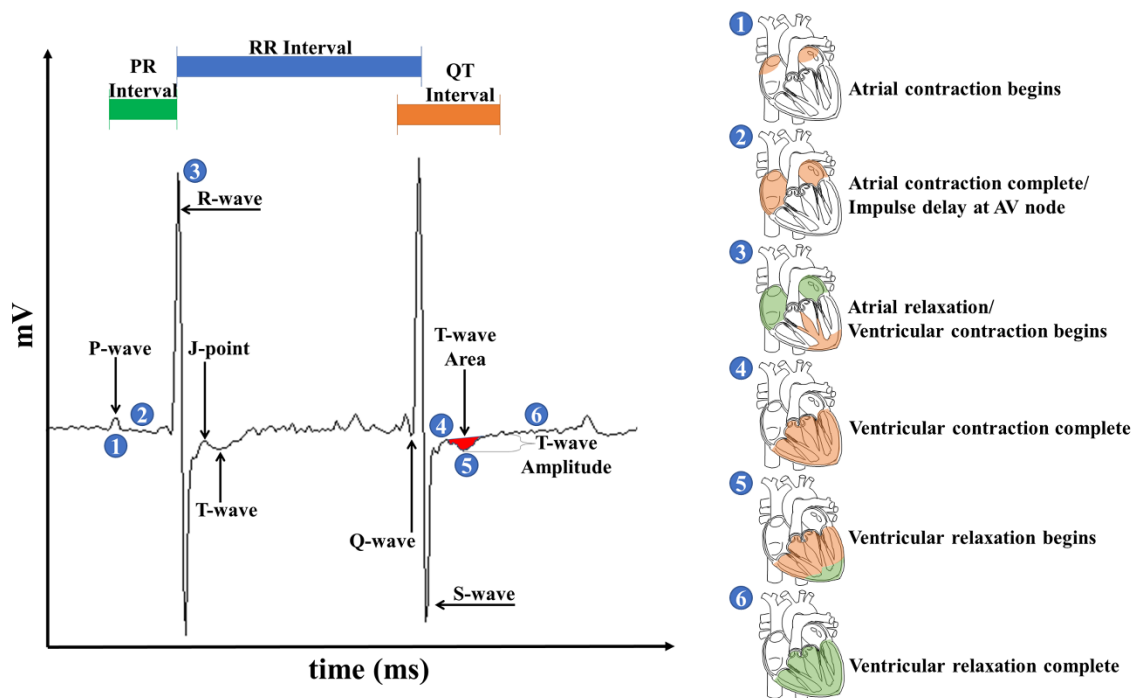


Figure 2. Idealized schematic of a typical ECG waveform and the cardiac cycle.

The series of cardiac cycle diagrams to the right of the waveform in Figure 2 show areas of the heart at key stages of a pulse corresponding to the number of the ECG waveform. The heart muscle phases through a contraction and relaxation cycle in response to the propagation of a wave of electrical signals initiated by pacemaker cells in the sinoatrial region of the heart. The light orange shaded areas in the cardiac cycle diagrams represent zones of contracting heart muscle, while the green shaded areas represent zones of the relaxing heart muscle.

All ECG and HRV parameters were acquired from freely moving, conscious mice and assessed at the same time every evening beginning at 6 hours following the exposure period (19:00 – 24:00). All waveforms were defined using ecgAUTO® software (EMKA Technologies S.A.S., Falls Church, VA, USA). As shown in Figure 2, the P-wave duration (1) corresponds to atrial depolarization while the PR interval (2) relates to the delay of the electrical impulse at the atrioventricular (AV) node and can be calculated as the time between the first deflections of the P-wave and QRS-wave complex. The QRS-wave complex (3) primarily represents the start of the ventricular depolarization and the end of atrial repolarization; the time interval between consecutive QRS-waves is defined as the R-R interval. The completion of ventricular depolarization following the QRS-wave (4) and the ventricular repolarization phase, known as the T-wave (5), occur almost instantaneously. The T-wave area was defined as the area over or under the ECG tracing from the peak of the J-wave (J-point) to the end of the T-wave, or where the T-wave returns to the isoelectric point. The T-wave amplitude was defined as the distance from the isoelectric line point of lowest deflection within the T-wave. The QT-interval encompasses the length of time from the onset of the Q-wave to the conclusion of the T-wave and corresponds to the ventricular repolarization phase and was measured and heart rate-corrected using Mitchell's correction (Mitchell et al. 1998). Ventricular repolarization is completed by the end of the T-wave and before the subsequent atrial depolarization (6). For this analysis, six ECG parameters were acquired: RR interval, PR interval, J-point amplitude, corrected QT interval, T-wave area, and T-wave amplitude (Boukens et al. 2014; Farraj et al. 2011; Goldberg et al. 1968; Speerschneider and Thomsen 2013).

#### *Heart Rate Variability*

Heart rate variability (HRV) was analyzed on ECG data recorded during the evening hours of 19:00 to 23:00 on each day after exposure. ECG data were assessed in 3-minute epochs every 30 minutes and analyzed for heart rate (HR) and normal beat-to-normal beat (N-N)-interval data which was then used to assess the magnitude of variance explained in the time-domain of the heart's rhythm as measured by SDNN (standard deviation of N-N intervals) and RMSSD (root mean squared of successive differences of N-N intervals). To assess frequency domain measures of HRV, periodicity of oscillations in heart rate were analyzed using Fast-Fourier transform (FFT) that separated the single ECG curve into its components made up of sinusoidal waves of specific frequencies (Rowan 2007). Frequency domain spectra were analyzed with resampling every 50ms and linear interpolation, in a 50% overlap with a Hamming window for segment lengths with 512 points (Thireau 2008, Fenske 2016). The power of the high-frequency (HF, 1.5-5.0 Hz) band has been used to represent cardiac vagal control which drives the parasympathetic nervous system (Fenske 2016, Liao 1996). The physiological interpretation of heart period oscillations at low frequency (LF, 0.04-0.15 Hz) are less well understood, and therefore are not reported (Camm 1996). Epochs were excluded if there was noise, or artifacts, in the ECG data acquisition, or an insufficient number of normal successive beats.

We evaluated HRV outcomes for evidence of exposure-related changes in terms of percent changes from baseline. To normalize for variability between individual mice, data were analyzed in terms of percent changes from baseline for each respective animal and averaged by exposure group and sex or treatment group.

## Reproductive Function Analyses

### *Estrous Cycling*

For evaluation of estrous cycling, mice were individually housed, and vaginal lavage was performed every morning using 0.9% NaCl for at least 14 days. Cells in the lavage fluid were examined by light microscopy immediately after collection, and the predominant cell types present in the fluid were recorded. Mice were euthanized on the day of proestrus of the cycle following exposures.

### *Ovarian Follicle Analysis*

The estrous cycle stage of the animal was assessed before harvesting the ovaries. Ovaries were embedded in glycolmethacrylate resin and sectioned at 20  $\mu\text{M}$ . Stereological methods were used to obtain unbiased estimates of ovarian follicle numbers (Charleston et al. 2007; Myers et al. 2004). Healthy follicles were classified as primordial (single layer of fusiform granulosa cells), primary (single layer with one or more cuboidal granulosa cells), secondary (greater than one layer of granulosa cells with no antrum), or antral (Lopez and Luderer 2004; Plowchalk et al. 1993). Ovarian follicles were counted blind to the treatment group using Stereo Investigator software (MBF Bioscience) with an Olympus BX40 light microscope equipped with 4 $\times$  UPlanFI, 10 $\times$  Plan, and 60 $\times$  PlanApo objectives, a joystick controller for a motorized XY stage (Ludl Electronic Products), and an Optronics MicroFire digital camera. We used the fractionator/optical dissector method to obtain unbiased and efficient estimates of primordial and primary follicle numbers by counting follicles in a defined fraction of the whole ovary (Myers et al. 2004). Three levels of sampling were used to determine the estimated number of primordial and primary follicles in the ovary. First, every 3rd section of the ovary was counted. For the second level of sampling, 2025  $\mu\text{m}^2$  counting frames were superimposed onto the sections in sampling grids that were subdivided into 8100  $\mu\text{m}^2$  squares. Follicles were counted if the oocyte fell within the counting frame and/or touched the inclusion boundaries and did not touch the exclusion boundaries. Lastly, the optical dissector height was set to 8  $\mu\text{m}$  with 2  $\mu\text{m}$  guard zones on the top and the bottom of the section to account for irregularities of the sections. Follicles were only counted if they were in focus within the optical dissector height. Sections were generally 13  $\mu\text{m}$  thick, and only 8  $\mu\text{m}$  fractions of the sections were counted. By multiplying the raw counts by the reciprocals of the fractions of the ovary counted, the number of follicles in the entire ovary can be estimated. Secondary, antral, and preovulatory follicles, ovulated oocytes, and corpora lutea were followed through every section to avoid counting any of these large structures more than once. The total number of healthy follicles or corpora lutea was calculated as the sum of the counts.

### *Immunohistochemistry*

Ovaries were fixed in 4% paraformaldehyde at 4°C, cryoprotected in 30% sucrose in PBS at 4°C, embedded in Optimal Cutting Temperature (OCT) compound, and stored at -80°C before being serially sectioned using a cryostat at a thickness of 10 $\mu\text{m}$ . Immunohistochemistry was performed using the Vectastain ABC kit (PK-4001; Vector Laboratories, Burlingame, CA, USA). Briefly, sections were thawed and heated for 15 min at 95°C in a 10mM citrate buffer (pH 6.0). The primary antibodies—rabbit anti-cleaved caspase-3 Asp 175 (1:100; Cell Signaling #9664, Beverly, MA, USA), rabbit anti-Ki67 (1:500; Abcam #15580, Cambridge, MA, USA) and rabbit anti- $\gamma\text{H2AX}$  (1:200; Cell Signaling #9718)—were detected using biotinylated goat anti-rabbit secondary antibody in 5% normal goat serum. All immunostaining procedures included avidin/biotin and 3% hydrogen peroxide blocking steps. Peroxidase activity was visualized using 3,3'-diaminobenzidine (DAB) as substrate (Roche). Sections were counterstained with hematoxylin. The following negative controls were included in every experiment:

secondary antibody without primary antibody; primary antibody without secondary antibody; and primary antibody replaced by rabbit IgG with secondary antibody. Both negative and positive follicles for each marker were counted, and quantities expressed as fractions were used for statistical analyses.

The numbers of Ki67, cleaved caspase-3, and phosphorylated histone 2AX ( $\gamma$ -H2AX, or gH2AX) -positive and -negative follicles or oocytes were counted in 3 or 4 slides per endpoint distributed throughout the ovary by an investigator blind to exposure group using an Olympus BX-60 microscope with 10, 20, and 40x U PLAN FLUO objectives equipped with a Retiga 2000R cooled CCD digital camera system with Q-Capture Pro software. The percentages of positive primordial and primary follicles (containing one or more positive granulosa cells per largest cross-section or containing positive oocytes) and secondary and antral follicles (containing three or more positive granulosa cells per largest cross-section or containing positive oocytes) were calculated and used for data presentation and analysis.

### *Surgery and Hormone Replacement*

Removal of the ovaries (ovariectomy) was performed on adult female apoE<sup>-/-</sup> mice. As a control, sham surgery was performed on another set of female mice. Ovariectomy is a procedure where ovaries are surgically excised and have been a valuable tool for understanding estrogen deficiency and procedures for the surgery have been described (Souza et al. 2019). The mice are first anesthetized using isoflurane. The hair is shaved off the flank area (between the last rib and above the pelvis), the skin is disinfected with chlorhexidine solution and an incision is made in the skin on the right side. The musculature is separated using curved tip scissors, the ovarian fat pad is pulled out of the incision, the region below the ovary is tightly clamped using a hemostat and the ovary is removed. The same steps are performed to remove the left ovary. The sham procedure is identical except for the ovary removal steps.

In a separate experiment, hormone replacement was performed on mice that had undergone surgery (ovariectomy or sham). At the time of surgery, either slow-release pellets containing 17  $\beta$ -estradiol (E2) or control pellets were implanted subcutaneously at the base of the neck (Innovative Research of America, Sarasota, FL). Based on previous studies, a 1.5 mg pellet was anticipated to result in estradiol levels in the 100pg/ml range in ovariectomized mice (Stormont et al. 2000), however the pellet would be expended before the end of the exposures. Therefore a second pellet (1 mg) was injected about midway through the exposure series. After recovery, a subset of mice then received telemetry implantation to collect ECG measurements during the experiment. For all animals, exposures to PM<sub>2.5</sub> or FA were initiated one week after surgery.

### *Echocardiogram Analysis*

In vivo cardiac function was assessed on the female animals that had undergone surgery from each cohort. Internal body temperature and stable heart rates of the animals were maintained under 1.5-2% isoflurane delivered through a nose cone. A 15 MHz probe was placed beside the sternum and above the heart in order to visualize the left ventricle, the mitral valve, and the aortic root of the rodent hearts. A series of two-dimensional images depicting the cardiac structures moving over time were captured. Three contraction/relaxation cycles of left ventricular performance were captured per mouse and used for data interpretation.

## Cardiomyocyte Analysis

Cardiomyocytes were isolated using retrograde perfusion techniques and placed in a perfused recording chamber on a microscope stage at roughly 37°C. Myocyte mechanics were assessed using video-based detection (IonOptix, Milton, Ma). Cells were visualized with a 40X objective on an inverted microscope and perfused with contractile buffer (in mol/L, pH 7.4): 131 NaCl, 4 KCl, 10 HEPES, 1 CaCl<sub>2</sub>, 1 MgCl<sub>2</sub>, and 10 glucose). The cells were field-stimulated at 1 Hz with 3-ms duration to detect functional properties of the cells (Monreal et al. 2008; Norby et al. 2002; Wold et al. 2002; Wold et al. 2003; Wold et al. 2012).

## Arterial Histology

Sections of the aortic root were collected, fixed, embedded, sectioned and stained with Oil Red-O and counterstained with hematoxylin/eosin to measure the degree of plaque formation.

## Statistics

### *Gravimetric and OC/EC Carbon Analysis*

Differences between the exposure group means were determined via SPSS® (IBM, Armonk, NY, USA) using one-way ANOVA corrected with Bonferroni's post-hoc adjustment. For data that are generally not represented by a normal distribution, such as counting data with small sample sizes which are often log-normally distributed, the non-parametric Kruskal-Wallis one-way ANOVA was applied. In all of the determinations, significance was assessed at  $P \leq 0.05$ .

### *ECG Measurements*

Baseline data between groups in each exposure period were compared by Student's two-tailed t-test with  $P \leq 0.05$  considered significant. Change from baseline measurements for ECG waveforms, HRV, and blood pressure between exposure group means were analyzed using Bonferroni-corrected two-way analysis of variance (ANOVA) for repeated measures. SPSS® (IBM, Armonk, NY, USA) was used for all statistical analyses. Normalcy of the data was checked using a Shapiro-Wilk test. Significance was assessed at  $P \leq 0.05$ .

### *HRV analysis*

Heart rate variability was analyzed via SPSS® (IBM, Armonk, NY, USA) using GLM-MANOVA models and linear mixed models corrected with Bonferroni's post-hoc adjustment, respectively. All homogenous subsets were identified using Tukey's post-hoc test with significance assessed at  $P \leq 0.05$ .

### *Echocardiography*

Echocardiographic assessments were read blind to treatment conditions. All collected data was analyzed using GLM-MANOVA models corrected with Bonferroni's post-hoc adjustment. All homogenous subsets were identified using Tukey's post-hoc test, with significance assessed at  $p \leq 0.05$ .

### *Lesion Characterization and Inflammatory Response*

Histology slides were read blind to treatment condition. The cellularity/unit area and the plaque area as a percent of arterial lumen were calculated. Lipid percentage was calculated as the percent of the plaque area that contained staining for lipids from the oil red O stain. Collagen percentage was

calculated as the percent of the plaque area that contained staining for collagen by Masson's Trichrome stain using NIH Image J software. An ANOVA was performed using SPSS to determine differences compared to controls with a significance level of  $p < 0.05$ .

#### *Cardiomyocyte Contractility*

Cardiomyocyte assessments were read blind to treatment conditions. All collected data was analyzed using GLM-MANOVA models corrected with Bonferroni's post hoc adjustment. All homogenous subsets were identified using Tukey's post-hoc test, with significance assessed at  $p \leq 0.05$ .

## Results and Discussion

### Comparison of Exposure-related Effects on Cardiopulmonary Physiology in Male and Female ApoE<sup>-/-</sup> Mice

We analyzed whether female mice that are genetically susceptible to developing atherosclerosis (apoE<sup>-/-</sup>) would be affected to a greater degree than similarly exposed male apoE<sup>-/-</sup> mice due to the adverse ovarian effects of PM<sub>2.5</sub> exposure. Thus, we analyzed responses in 4 experimental groups of mice: (1) purified Air-exposed males, (2) CAPs-exposed males, (3) purified Air-exposed females, and (4) CAPs-exposed females.

#### *Particle Concentrations*

Number and mass concentrations of exposure atmospheres averaged over the 12-week exposure period are summarized in Table 1. The VACES concentrated PM<sub>2.5</sub> by an average of 8.5 times the ambient level. The particle size distributions of the CAPs atmospheres were not significantly different from that of the ambient particles. The average CAPs exposure was 130 µg/m<sup>3</sup> averaged over the 5-hr exposure session, a level which is well within the limits of peak exposures measured in California, and in the range of average exposures in more polluted parts of the world. Also note that while the CAPs exposures were high, relative to the current 24-hr National Ambient Air Quality Standard (35 µg/m<sup>3</sup>), our exposures were for 5 hours per day, which would be an equivalent exposure of 27 µg/m<sup>3</sup> if averaged over the entire day.

*Table 1. Concentrations Averaged Over Exposure Period*

	Particle Number (cm <sup>-3</sup> )	Particle Mass (µg m <sup>-3</sup> )
Purified Air	10 ± 20	≤ 5
Ambient Air	(1.0 ± 0.1) × 10 <sup>4</sup>	18 ± 2
PM <sub>2.5</sub> CAPs	(0.95 ± 0.2) × 10 <sup>5</sup>	130 ± 5

#### *Electrocardiography: Rate-Associated Endpoints*

A subset of male and female mice from each group were implanted with telemetry devices for the acquisition of ECG measurements. Heart rate-dependent ECG parameters measured in these mice are shown in Figure 3. In comparison to sex-matched controls, exposure to CAPs appeared to affect males more than females. In fact, male mice exposed to CAPs exhibited consistent differences in the PR interval and the QRS interval changes compared to male mice exposed to air. On the ECG, the PR interval begins with atrial depolarization (contraction) and ends with the commencement of ventricular depolarization (contraction), which is triggered by the impulse from the AV node (Figure 2). The QRS interval represents ventricular depolarization (Figure 2). Figure 3 shows that CAPs-exposed males generally had a greater increase in the PR interval compared to controls for each week of the study. In addition, while CAPs-exposed males experienced significant differences in the QRS interval compared to

air-exposed males, there were no significant differences between the female groups (Figure 3). Altogether, the CAPs-exposed males may be more susceptible to atrial conduction anomalies as indicated by a significant P-R interval elongation, with corresponding shorter QRS intervals compared to those observed in air-exposed controls. It is also worth noting that with the male mice, while there were week-to-week variations, the changes were not progressive, i.e. the diversions did not, apparently, differ markedly with time (or with animal age).

On the other hand, some responses did vary with time, rather than with exposure, in female mice. In general, there were no exposure-related changes related to atrial function in the female mice. However, during the last 5 weeks of the study in both CAPs-exposed and air-exposed female mice, there were increases in heart rate and QTcB interval. The observed shift was possibly due to the effect of chronic exposure or was possibly age-related.

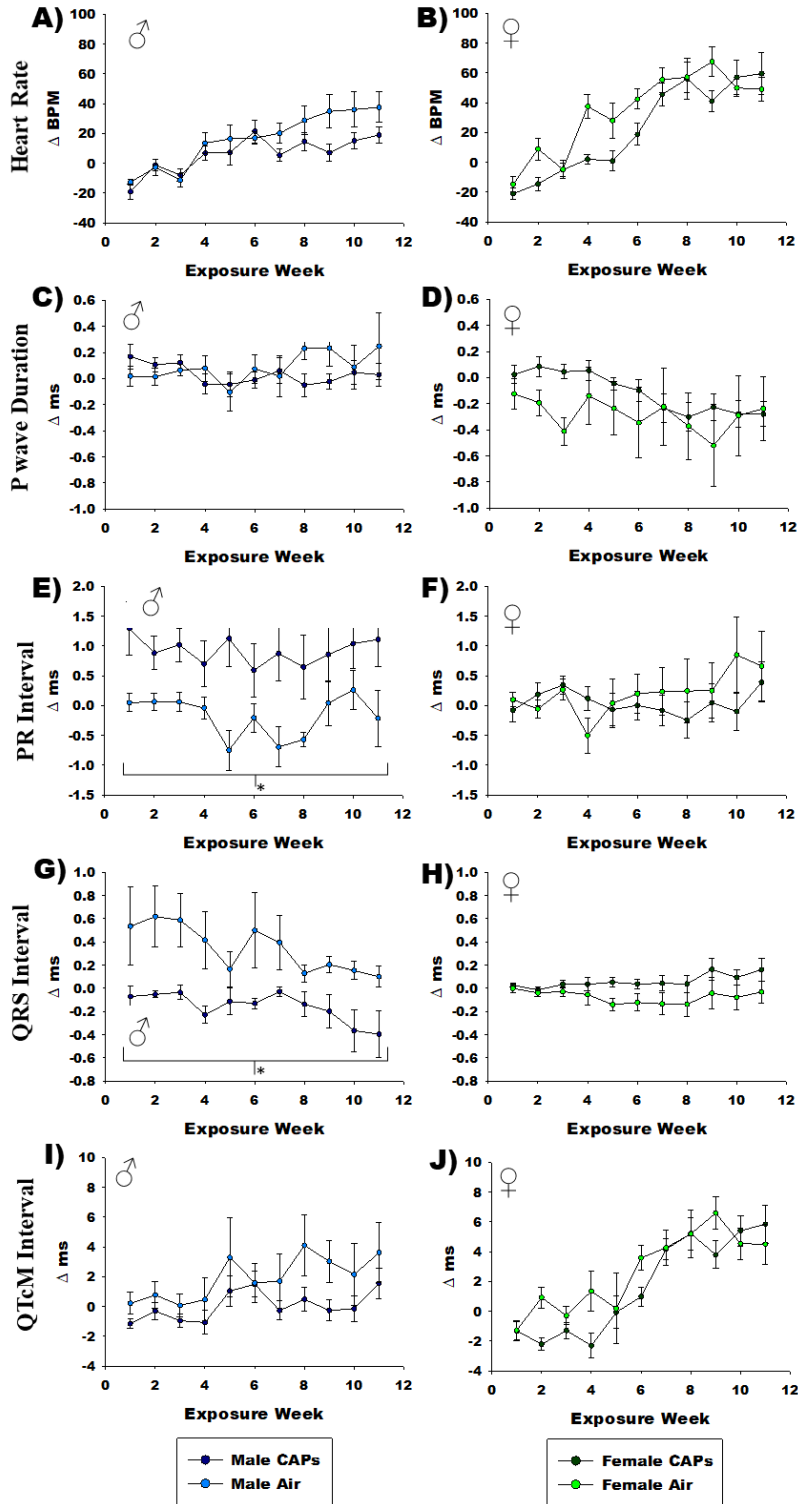


Figure 3. Sex-dependent responses in heart rate-related ECG waveform parameters.

A) and B) Male and female heart rate; C) and D) Male and female P-wave duration; E) and F) Male and female PR interval; G) and H) Male and female QRS duration; and I) and J) Male and Female QTcM interval. The plots display responses in CAPS- and Air-exposed mice over the exposure period as the change in value from baseline (week 0) (Mean  $\pm$  SE;  $n=5$ /group). Heart rate is plotted as the change in beats-per-minute ( $\Delta$  BPM). P-wave duration, PR-Int, QRS-Int, and QTcM (corrected QT) interval are plotted as the change in milliseconds ( $\Delta$  ms). \* $p \leq 0.05$ .

### Electrocardiography: Ventricular-Associated Endpoints

Chronic exposure to CAPs produced sex-dependent changes in ventricular conduction-associated parameters including T-wave amplitudes and T-wave area, which are summarized in Figure 4. As Figure 2 shows, the time beginning from the J-point and moving through the T-wave encompasses ventricular repolarization (relaxation). We saw no changes in J-point levels in both male and female mice exposed to CAPs throughout the exposure period (Figure 4). However, CAPs exposure appeared to affect the T-wave amplitude and T-wave area in females differently than did filtered air exposure. Though insignificant, control females generally showed increases in these values throughout the exposure period compared to reductions or smaller magnitude changes in the CAPs-exposed females (Figure 4). These effects on the T-wave did not occur in the male groups. Overall, alterations in T-wave characteristics possibly indicate issues with ventricular repolarization.

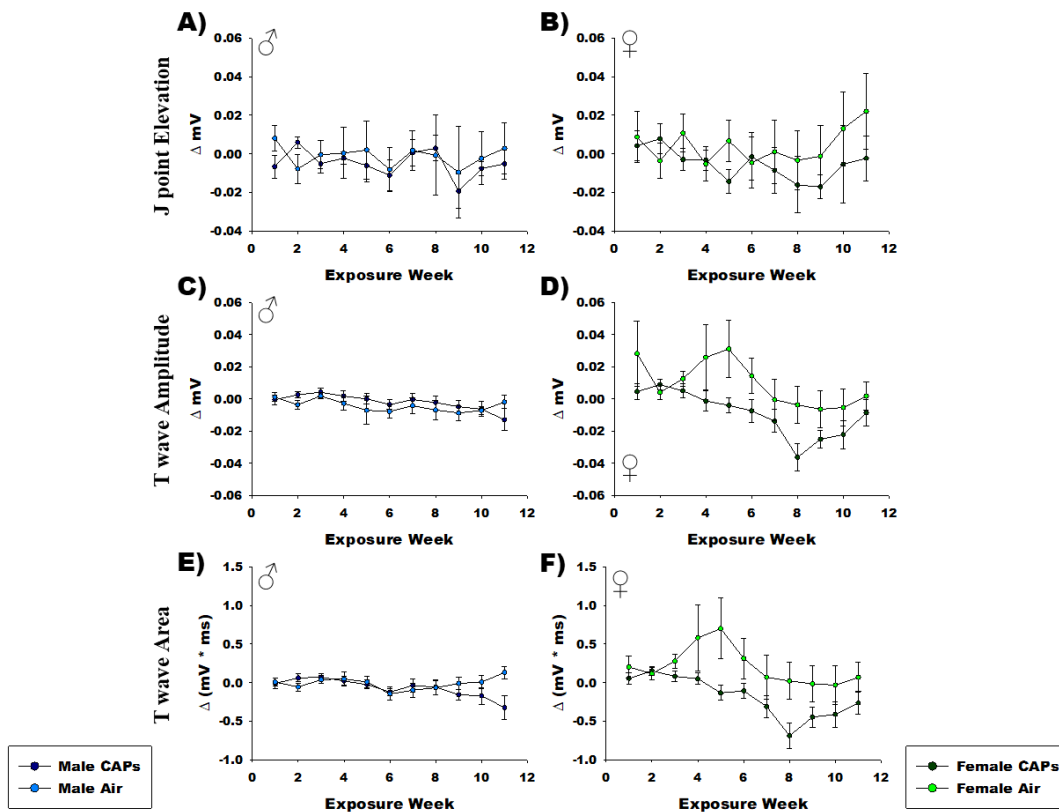


Figure 4. Sex-dependent responses in ventricular-function-related electrocardiographic wave form parameters.

A) and B) Male and female J point elevation; C) and D) Male and Female T wave amplitude; E) and F) Male and Female T wave area. The plots display responses in CAPs- and air-exposed mice over the exposure period as the change in value from baseline (week 0) (Mean  $\pm$  SE; n=5/group). J point elevation and T wave amplitude are plotted as the change in millivolts ( $\Delta$  mV). T wave area is plotted as the change in the product of millivolts multiplied by milliseconds ( $\Delta$  (mV \* ms)).

### *Heart Rate Variability*

HR and time-domain HRV measures (SDNN and RMSSD) are displayed in Figure 5 and Table 2. SDNN is a general measurement of the total variability of the interval between beats, while RMSSD is a measure of the parasympathetic response. It is worth noting that the acute responses, within the first 3 weeks of the exposures, do not represent the chronic effects of inhalation exposure to CAPs in males nor females. Figure 5 illustrates that over the course of the exposure period, there was a general tendency for decreased HRV in CAPs-exposed mice, and that there were differences between males and females. In females, chronic exposure to CAPs resulted in a trend towards a decrease of SDNN (Table 2). On the other hand, the male groups displayed large inter-animal variability for SDNN, and thus no pattern emerged here. Despite differences in HR and SDNN trends, males and females had similar direction and magnitude of change in RMSSD after CAPs exposure. Decreases in RMSSD in both males and females reflect changes to parasympathetic nervous system inputs to the heart after chronic air pollution exposure.

Most studies of HRV focus on relatively short exposures, a few hours to a few weeks. Our study demonstrates that HR and HRV measures change from the initial few weeks of exposure to several weeks later, demonstrating the need for chronic exposure studies to more fully understand the potential for negative health outcomes. Overall, sex-differences are evident in CAPs-induced HRV changes, with females showing a greater negative HRV response to CAPs exposure than do males, highlighting sex-differences in cardiovascular effects of PM inhalation.

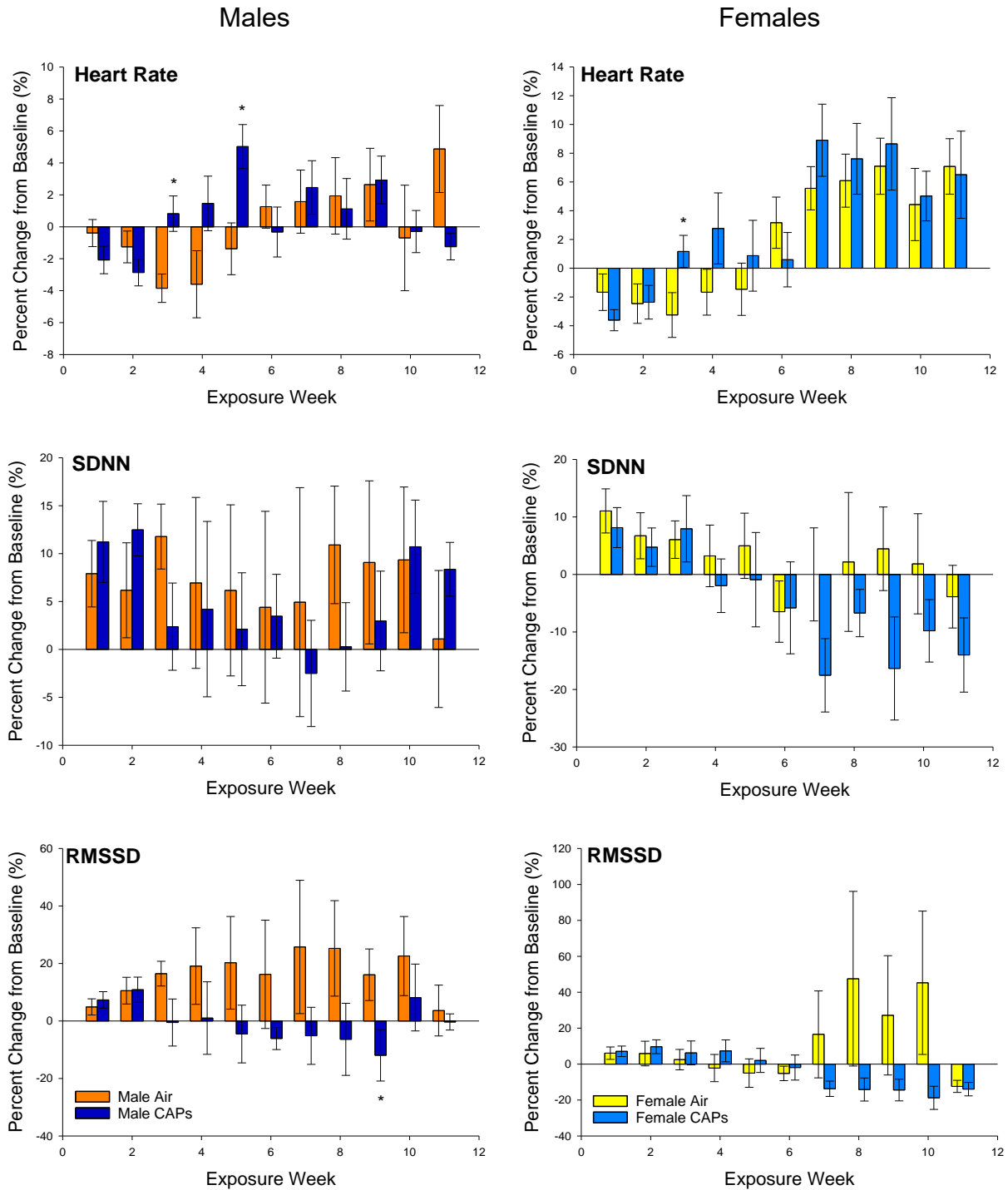


Figure 5. Sex-dependent responses in HRV.

The left-hand plots display responses in CAPs- and air-exposed males over the 12-week exposure period, while the right-hand plots show responses in the female groups (Mean  $\pm$  SE; n=5/group). The plots show the percent change in value from baseline (week 0). SDNN = Standard Deviation of NN interval; RMSSD = Root Mean Squares of Successive Differences of NN intervals). Statistical analyses of the final 5 weeks of the exposure are in Table 2. \* $p \leq 0.05$  compared with air-exposed of the same exposure week.

Table 2. Average and standard error of HR, SDNN and RMSSD of pooled change from baseline during the final 5 weeks of the exposure (weeks 7-11 from Figure 5).

		Male			Female		
		Air	CAPs	p-value	Air	CAPs	p-value
HR	<i>bpm</i>	2.0 ± 1.1	1.0 ± 0.7	NS	6.1 ± 0.9	7.3 ± 1.1	NS
SDNN	<i>ms</i>	7.0 ± 3.9	4.0 ± 2.1	NS	0.9 ± 3.7	-12.9 ± 2.8 *	0.018
RMSSD	<i>ms</i>	19.0 ± 7.1	-3.1 ± 4.3	0.52	24.8 ± 14.8	-15.0 ± 2.4 *	0.016

\*p<0.05. All statistical analyses performed were general linear models with a Bonferroni correction of multiple comparisons using all data points for each animal's daily HRV measures throughout the specified averaging time.

### Blood Pressure

Blood pressure at systole (cardiac contraction) and diastole (cardiac relaxation) were measured via implanted pressure transducer located in the left common carotid arteries of a subset of exposed animals. CAPs-exposed males exhibited consistent decreases in systolic and diastolic blood pressure (Figure 6A and 6C), but they were not statistically significantly different from those measured in Air-exposed mice. On the other hand, both systolic and diastolic blood pressures were increased in CAPs-exposed female mice compared to that in Air-exposed females (Figure 6B and 6D). In fact, the differences between blood pressures in CAPs-exposed vs. Air-exposed females increased progressively over the exposure period and were consistent with the decrease in heart rate (Figure 5) and breathing rate (Figure 7), which altogether would allow for maintaining homeostatic control of cardiac ejection fraction and delivery of oxygenated blood from the heart. The changes in blood pressure and heart rate, from weeks 7-12, were also accompanied with significant changes in HRV, as described earlier (Figure 5 and Table 2).

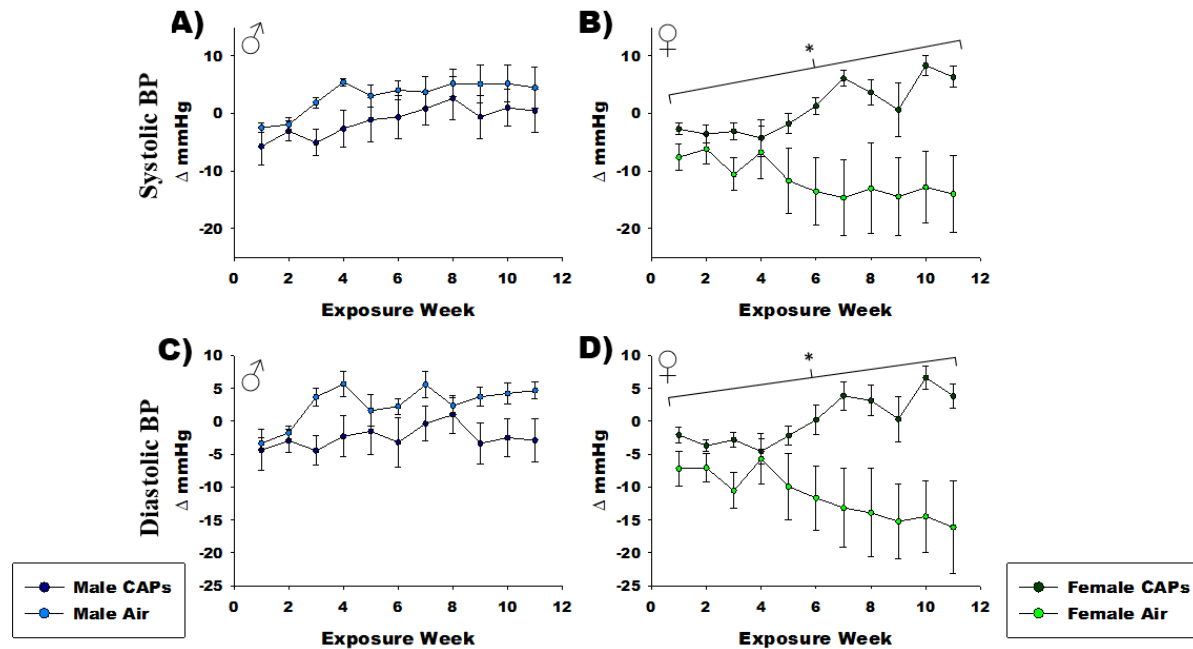


Figure 6. Sex-dependent changes from baseline systolic and diastolic blood pressures (BP).

A) and B) Male and female systolic BP; C) and D) Male and female diastolic BP. The plots display responses in CAPs- and air-exposed mice over the exposure period as the change in value from baseline (week 0) (Mean  $\pm$  SE; n=4-5/group). Systolic and diastolic BP are plotted as the change in millimeters of mercury ( $\Delta$  mmHg). \* $p \leq 0.05$ .

### Cardiopulmonary Function Measurements

Other measures that indicate the cardiopulmonary status of our animals were also analyzed. Since the heart pumps oxygenated blood through the aorta for distribution to the rest of the body, we calculated the rate of change in pressure in the aortic arch over time (dP/dt) using measurements from the pressure catheter implanted in the left common artery of the mice. Exposure to CAPs did not alter the dP/dt in either sex, over the course of the exposures, as compared to Air-exposed mice, which is an indication that left ventricular contractility was not adversely affected by the exposures (Figure 7A and 7B). We also calculated the rate-pressure product (Rate  $\times$  Pressure, or RPP), which is the product of the heart rate and systolic blood pressure and is used clinically as a surrogate measure of the heart's ability to satisfy myocardial oxygen demand. Male mice did not show any exposure-based alterations in the RPP over the course of the exposure (Figure 7C) while CAPs-exposed female mice began to increase over control levels starting halfway through the exposure period (Figure 7D), possibly indicating a systemic cumulative effect of PM exposure. But since nearly all of the significant effects were seen in female mice, the effects may also be related to changes in the ovaries which were measured at the end of the 12-week exposure and are shown in Figures 8-12.

We were also able to evaluate effects on breathing rate, which is another key measure of cardiopulmonary function, by evaluating the pressure modulation induced by respiration and superimposed on the blood pressure waveform. The ecgAUTO software extracts breathing rates from measurements recorded with the implanted blood pressure catheter. There were sex differences in the effect of CAPs on breathing rate. The breathing rate (breaths per minute) was unchanged over the exposure period in male mice after PM exposure (Figure 7E) but was significantly decreased ( $p \leq 0.05$ ) in

CAPs-exposed females compared to air controls over the entire exposure period (Figure 7F). Breathing rate in males decreased slightly, but not significantly, over time in air- and CAPs-exposed males, but progressively increased significantly ( $p \leq 0.01$ ) in both CAPs (19% per week) and air-exposed (6% per week) females. The breathing rate increase in CAPs-exposed females could be compensatory for the decrease in myocardial oxygen delivery, as indicated by the decreased RPP in this cohort.

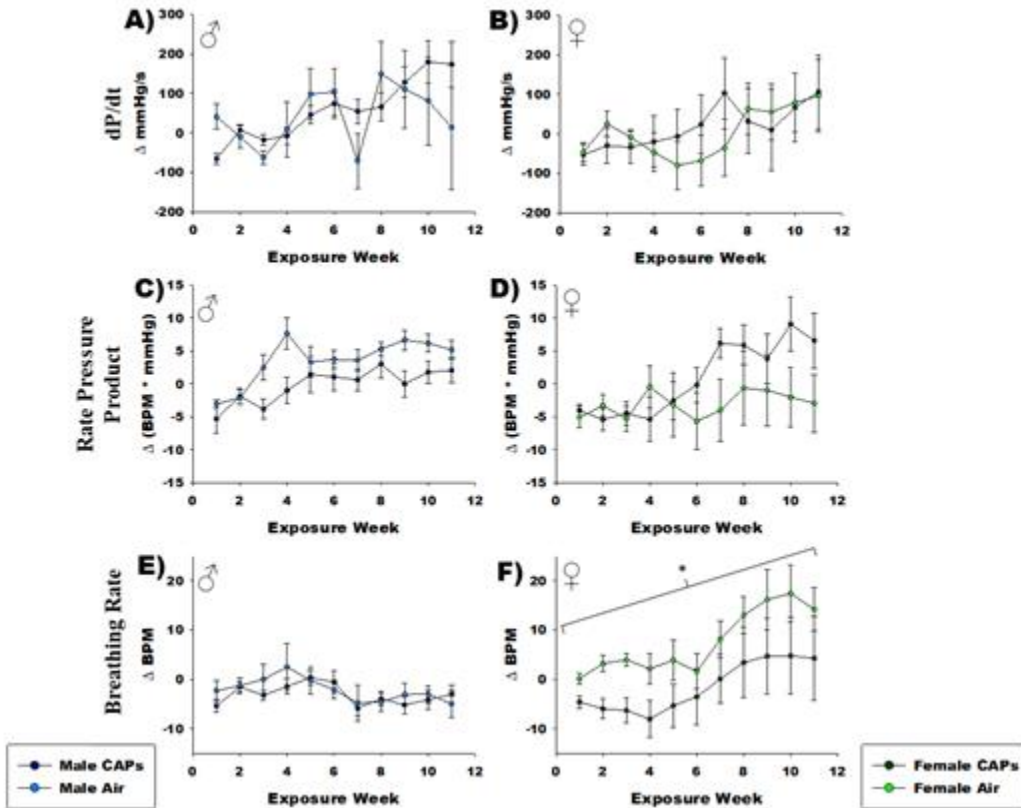


Figure 7. Sex-related differences in cardiopulmonary function measurements.

A) and B) Male and female change in pressure over change in time (dP/dt); C) and D) Male and female rate pressure product; E) and F) Male and female breathing rate. The plots display responses in CAPs- and air-exposed mice over the 12-week exposure period as the change in value from baseline (week 0) (Mean  $\pm$  SE; n=5/group). dP/dt is plotted as the change in millimeters of mercury per second ( $\Delta$  mmHg/s). The Rate Pressure Product is plotted as the change in breaths per minute multiplied by millimeters of mercury ( $\Delta$  (BPM x mmHg)). Breathing rate is plotted as the change in breaths per minute ( $\Delta$  BPM). \* $p \leq 0.05$ .

## Effects of CAPs Exposure on Ovariectomized and Intact ApoE<sup>-/-</sup> Mice

We have demonstrated that female mice respond to PM<sub>2.5</sub> exposure differently than males in terms of some various cardiopulmonary measures. To follow up on these findings, we analyzed whether there were any effects on the ovaries of the female mice and further whether loss of ovarian function, through ovariectomy, would affect the susceptibility of female mice to the cardiovascular effects of PM<sub>2.5</sub> exposure. For effects on the ovaries, we compared two female groups: (1) air-exposed, and (2) CAPs-exposed. For the experiment looking at the role of ovarian function, we compared 4 experimental female groups: (1) air-exposed, sham surgery; (2) CAPs-exposed, sham surgery; (3) air-exposed, ovariectomized (OVX); and (4) CAPs-exposed, OVX.

### Exposure Data

The experimental exposure conditions are shown in Table 3. The average concentration of CAPs was 6.3 times greater than concentrations measured in ambient air for the entire exposure. The PM<sub>2.5</sub> mass concentration levels during the 12-week exposure period were concentrated 8.5-fold over ambient levels.

Table 3. Concentrations Averaged Over Exposure Period

	Particle Number (cm <sup>-3</sup> )	Particle Mass (µg m <sup>-3</sup> )
Purified Air	≤ 20	≤ 5
Ambient Air	(1.8 ± 0.1) × 10 <sup>4</sup>	30 ± 2
PM <sub>2.5</sub> CAPs	(0.90 ± 0.2) × 10 <sup>5</sup>	125 ± 5

### Effects of CAPs Exposure on Ovaries in Female ApoE<sup>-/-</sup> Mice

The ovaries contain a finite follicular pool. Ovarian follicles progress from a primordial stage through primary, secondary, antral, and finally pre-ovulatory stages. The life cycle of a follicle ends upon ovulation, whereby the pre-ovulatory follicle ruptures to release an oocyte. The finite pool of primordial follicles constitutes the total ovarian follicle reserve, from birth. We found that exposure to PM<sub>2.5</sub> CAPs depleted the follicular pool. Primordial follicle counts were reduced by 40% with CAPs exposure, although this was not significant (p=0.13) (Figure 8). However, primary follicle counts significantly decreased by 53% (p=0.007) (Figure 8), and healthy secondary follicle counts per ovary were also significantly reduced (p=0.04) (Figure 9). Since antral follicles produce estradiol in response to gonadotropin hormones produced by the anterior pituitary, we also quantified these. However, CAPs did not affect counts of healthy antral follicles or atretic follicles (Figure 9).

The main mechanisms by which the ovarian follicle pool can be prematurely depleted is by increased follicle death, by accelerated recruitment of primordial follicles into the growing pool, or by a combination of the two. Immunostaining for Ki67, a cell proliferation marker, was performed to determine if accelerated recruitment was occurring. As seen in Figure 10, the percentage of primordial follicles with Ki67-positive granulosa cells was non-significantly increased, and the percentage of primary follicles that had Ki67-positive granulosa cells did not change significantly in PM<sub>2.5</sub>-exposed mice. Thus, there was no statistically significant accelerated recruitment of primordial follicles.

A cause of follicle depletion could be increased apoptosis (cell death). Thus, sections were stained for the apoptotic marker caspase 3 to determine if this was occurring. As shown in Figure 11, exposure to PM<sub>2.5</sub> does not affect caspase 3 activation in ovarian follicles. The percentages of histologically healthy plus atretic secondary and antral follicles that had activated caspase 3-positive granulosa cells increased slightly, but non-significantly, in mice exposed to PM<sub>2.5</sub> for 12 weeks (P=0.17 by Kruskal Wallis test). No caspase 3-positive primordial follicles and very few positive primary follicles were noted (not shown, N=6-7/group).

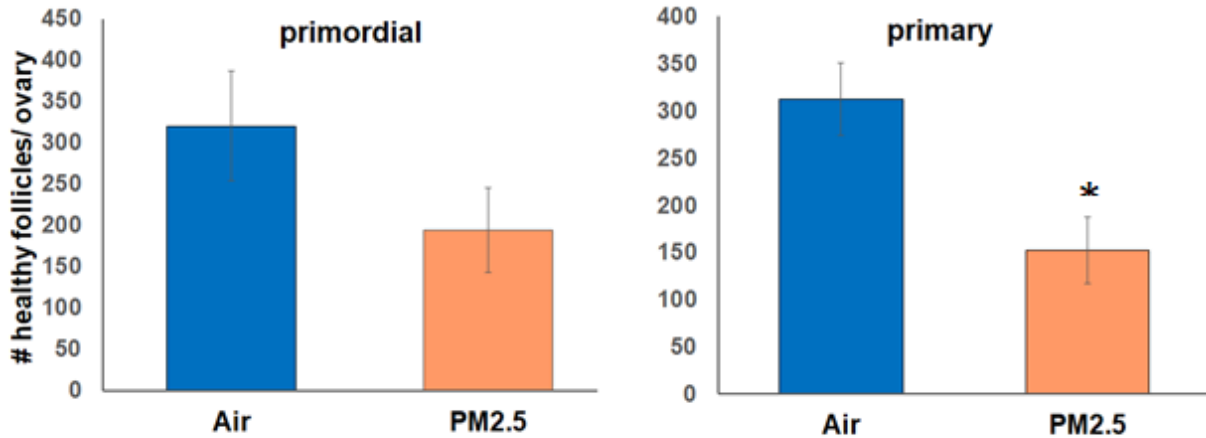


Figure 8. Primordial and primary follicle numbers per ovary. Follicle numbers were estimated for the air- and PM<sub>2.5</sub>-exposed females (N=10/group) using nonbiased stereological methods. \*p=0.007 compared with air-exposed, via t-test.

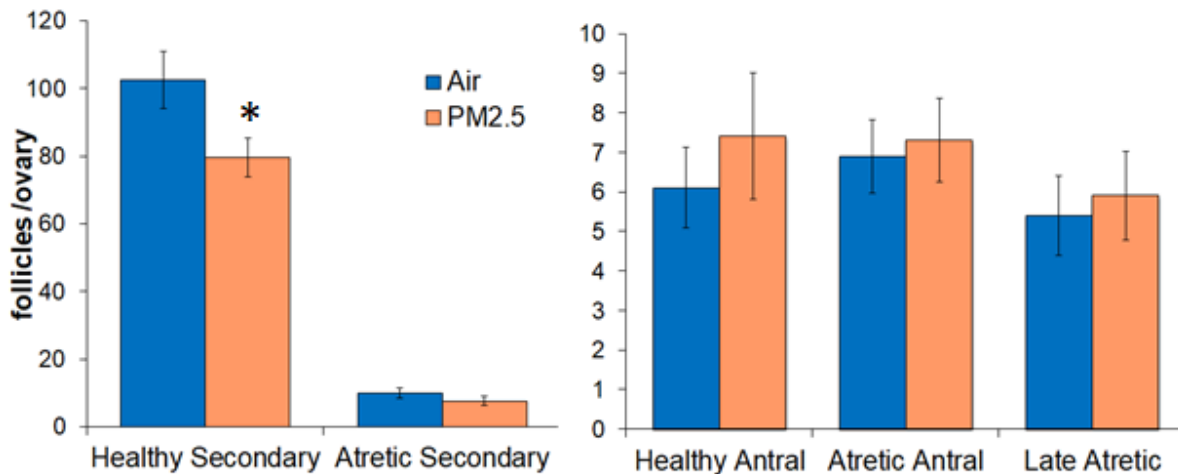


Figure 9. Healthy and atretic secondary and antral follicles. Healthy and atretic secondary and antral follicles for the air- and PM<sub>2.5</sub>-exposed females (N=10/group) were followed through every serial section to avoid over counting. \*p=0.04 compared with air-exposed, via t-test.

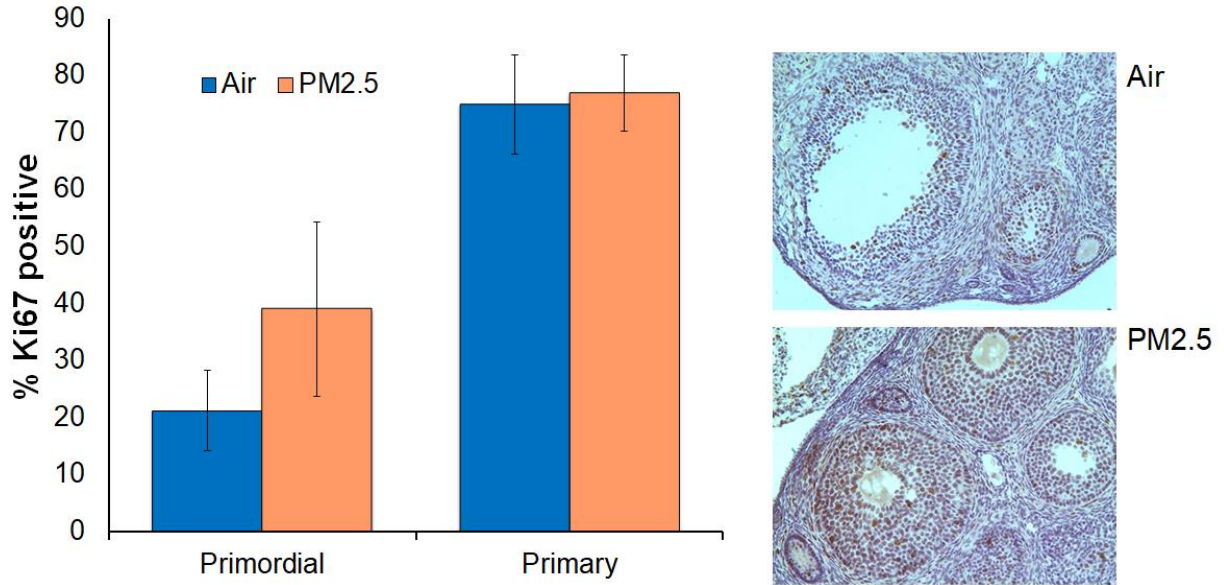


Figure 10. *Ki67-positive granulosa cells in primordial and primary follicles.*

The percentages of primordial and primary follicles that had Ki67-positive granulosa cells (brown staining) did not increase significantly in mice exposed to PM<sub>2.5</sub> for 12 weeks ( $p>0.4$  by Kruskal-Wallis test). As expected, secondary and antral follicles were all positive for Ki67 (summary data not shown). For example, large follicles at top and lower left in PM<sub>2.5</sub> image are antral follicles, while small follicle at lower left is a small secondary follicle.  $n=6$ /group.

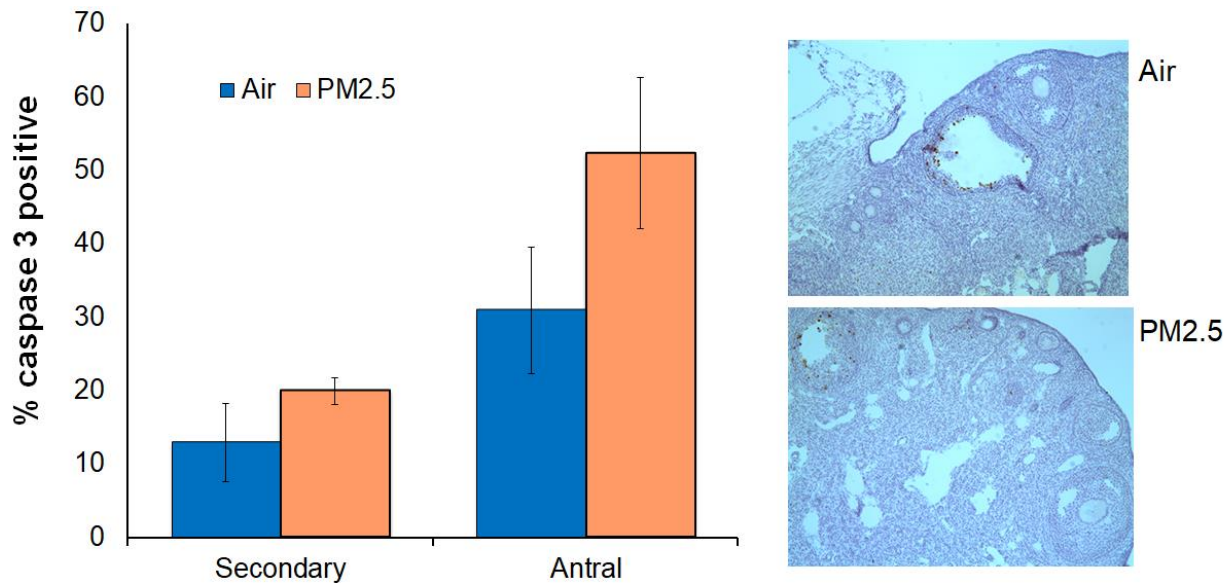


Figure 11. *Caspase-3-positive granulosa cells in secondary and antral follicles.*

The percentages of histologically healthy plus atretic secondary and antral follicles that had activated caspase 3 positive granulosa cells increased slightly, but non-significantly, in mice exposed to PM<sub>2.5</sub> for 12 weeks ( $P=0.17$  by Kruskal Wallis test). Large follicles at top middle of the Air photomicrograph and top left of the PM<sub>2.5</sub> micrograph are atretic antral follicles with activated caspase 3 positive (brown staining) granulosa cells. No caspase 3 positive primordial follicles and very few positive primary follicles were noted (not shown).  $N=6-7$ /group.

Increased levels of phosphorylated histone 2AX (gH2AX) in ovarian cells are also associated with decreased cell viability and increased apoptosis. As shown in Figure 12, there was a statistically significant increase in the percentage of primary follicles with gH2AX positive granulosa cells in PM<sub>2.5</sub> exposed compared to controls (P=0.008, Kruskal Wallis test). Percentage of primary follicles with gH2AX positive oocytes was non-significantly increased (P=0.115). Percentage of secondary follicles with gH2AX positive oocytes was also non-significantly increased (P=0.152). Percentages of primordial follicles with gH2AX positive oocytes (P=0.317) and granulosa cells (P=0.355) were non-significantly increased. Antral follicles are mostly positive in both groups.

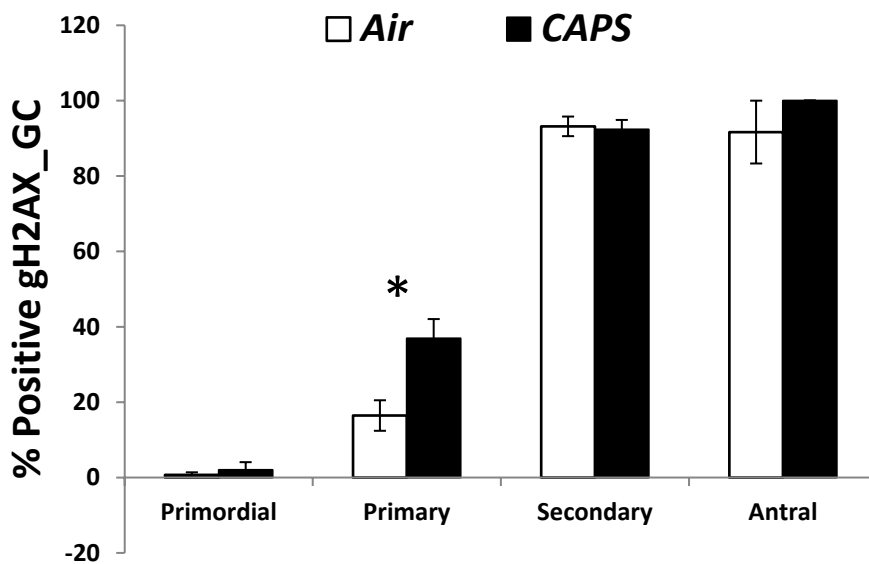


Figure 12. Percentage of follicles with granulosa cells (GC) that stained positively for gH2AX. \*p<0.05

### *Electrocardiography: Rate-Related Endpoints*

Chronic exposure to CAPs did not alter the heart rate of intact CAPs-exposed animals compared to air-controls (Figure 13). There was a trend toward increased heart rates seen in the CAPs-exposed ovariectomized (OVX) animals compared to controls for the duration of the exposure. The OVX cohort also experienced large RR interval deviations during the last three weeks of the exposure. The atrial depolarization rate (P wave duration) was increased in the CAPs-exposed SHAM animals compared to controls. Conversely, OVX animals exposed to CAPs exhibited a trending decrease in P-wave duration. Interestingly, we did observe a significant decrease in P wave duration between the SHAM and OVX control groups, highlighting the potential involvement of circulating ovarian hormones in normal cardiac function. Atrial repolarization (PR Interval) was not affected by CAPs exposure in SHAM animals. A trend towards decreased relaxation rates compared to controls was seen in the OVX group. The ventricular depolarization rate (QRS Interval) was not affected by CAPs exposure in either the SHAM or OVX treatment groups. However, we did observe a trend toward decreased ventricular repolarization rates (QTcM Interval) in the CAPs-exposed OVX animals compared to controls. This response was similar to that seen in the heart rates of CAPs-exposed OVX animals suggesting that the decreased heart rate is driven by changes in ventricular repolarization. These results suggest that exposure to PM is capable of impairing cardiac conduction rates. Furthermore, removing circulating ovarian hormones can potentially alter the physiologic responses to PM inhalation.

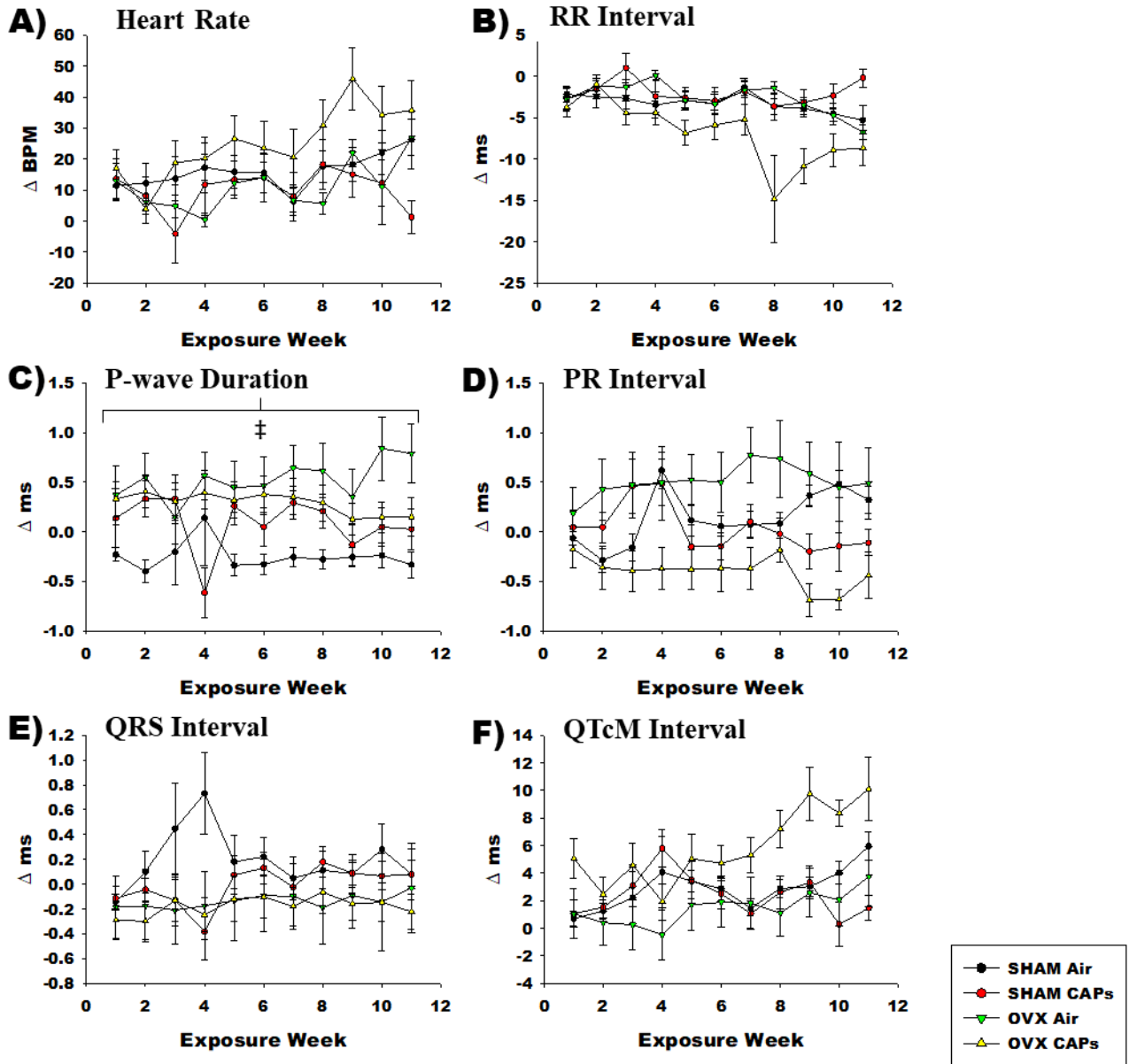


Figure 13. Rate-related ECG endpoints: OVX vs SHAM.

A) Heart rate; B) RR Interval; C) P-wave duration; D) PR interval; E) QRS interval; F) QTcM Interval. The plots display responses over the 12-week exposure period in female mice who were either ovariectomized (OVX) or underwent sham surgery (Mean  $\pm$  SE; n=4-5/group). The plots show the change in value from baseline (week 0). Heart rate is plotted as the change in beats-per-minute ( $\Delta$  BPM). R-R interval, P-wave duration, P-R interval, QRS interval, and corrected Q-T interval are plotted as the change in milliseconds ( $\Delta$  ms). #Sham Air vs. OVX Air at  $P \leq 0.05$

### Electrocardiography: Ventricular-Related Endpoints

Exposure-related ECG changes were seen for parameters associated with ventricular functions (Figure 14). CAPs exposure significantly ( $p \leq 0.05$ ) increased T wave areas and T wave amplitudes in OVX mice, compared to that measured in air-exposed OVX mice. J point elevations were not consistently different between CAPs-exposed OVX animals and air-exposed OVX animals. No exposure-related differences were seen in intact (Sham-operated) mice with respect to J point elevation, T wave area or T wave amplitude.

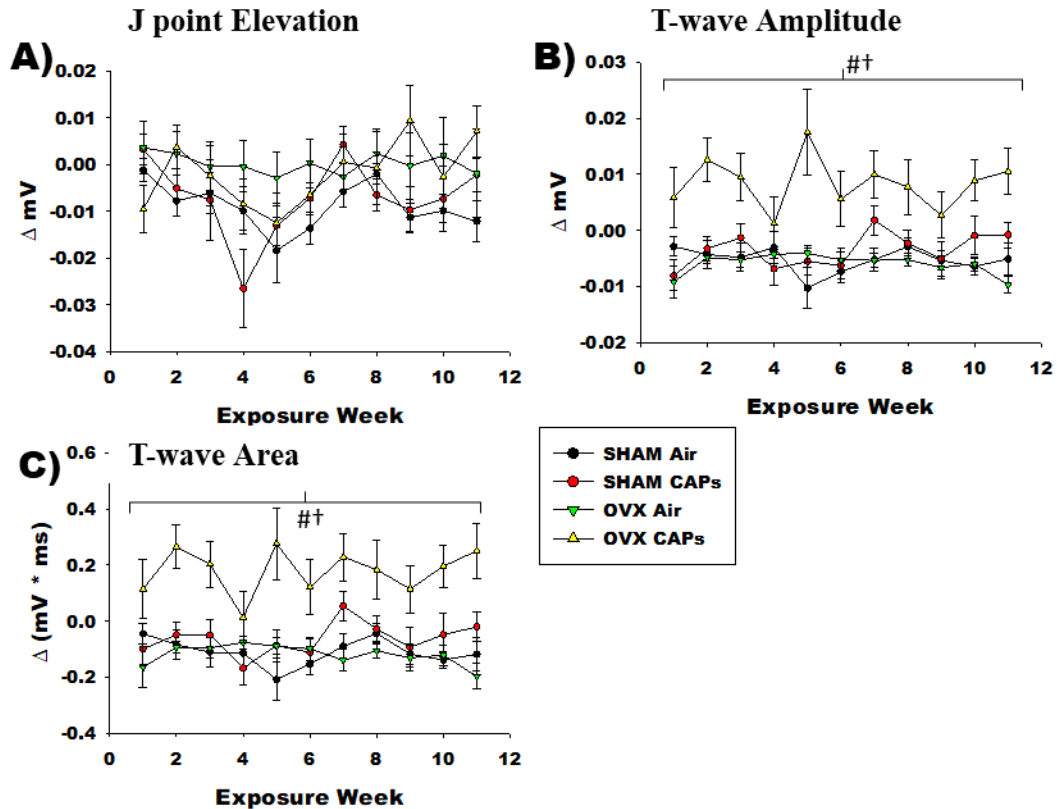


Figure 14. Ventricular-related ECG endpoints: OVX vs. SHAM. A) J-point elevation; B) T-wave Amplitude; C) T-wave Area. The plots display responses over the 12-week exposure period in female mice who were either ovariectomized (OVX) or underwent sham surgery (Mean  $\pm$  SE; n=4-5/group). The plots show the change in value from baseline (week 0). J-point elevation and T wave amplitude are plotted as the change in millivolts ( $\Delta$  mV). T wave area is plotted as the change in the product of milliseconds multiplied by millivolts ( $\Delta$  (ms \* mV)). \*Sham CAPs vs. OVX CAPs at  $P \leq 0.05$ ; #OVX CAPs vs. OVX Air at  $P \leq 0.05$

### Heart Rate Variability

Increased heart rates and decreased R-R intervals were measured in all cohorts over the course of the exposure (Figure 15). However, exposure to CAPs induced greater increases compared to controls with larger deviations seen in the intact animals. Exposure to CAPs also produced a trending decrease in SDNN and RMSSD in the intact animals while no effect was seen in the OVX animals for either measure.

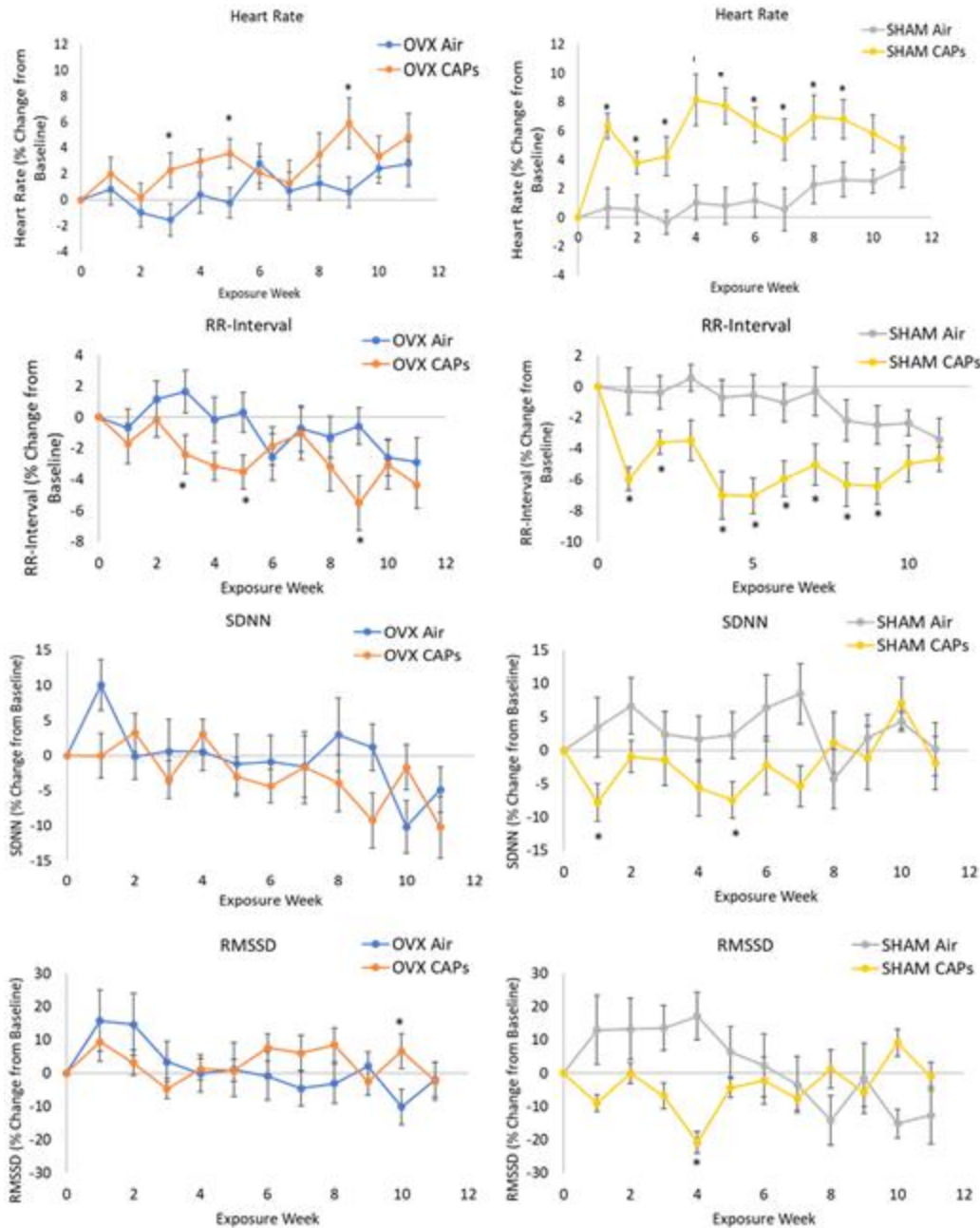


Figure 15. Time-domain parameters of heart rate variability (HRV)

HRV parameters were measured in the evening of each day of CAPs or Air exposure and averaged for each week for ovariectomized (OVX) and non-ovariectomized mice that underwent a sham surgery (SHAM). Note: n=4-5 per group; \*p < 0.05.

Frequency-domain measures of HRV (high frequency, HF, and low frequency, LF) were additionally quantified. HRV is controlled by the sympathetic and parasympathetic nervous systems, and the HF values represent parasympathetic control. LF values are less well-understood, however we have calculated and analyzed the ratio of LF/HF in Figure 16. Exposure to CAPs moderately decreased measures of high frequency HRV at the beginning of the exposure period compared to controls in only the intact animals (Figure 16). No changes were seen in the OVX cohort. There was no effect of CAPs exposure on the LF/HF ratio in either ovariectomy treatment group, but when compared within the exposure atmosphere groups, ovariectomy decreased the LF/HF ratio.

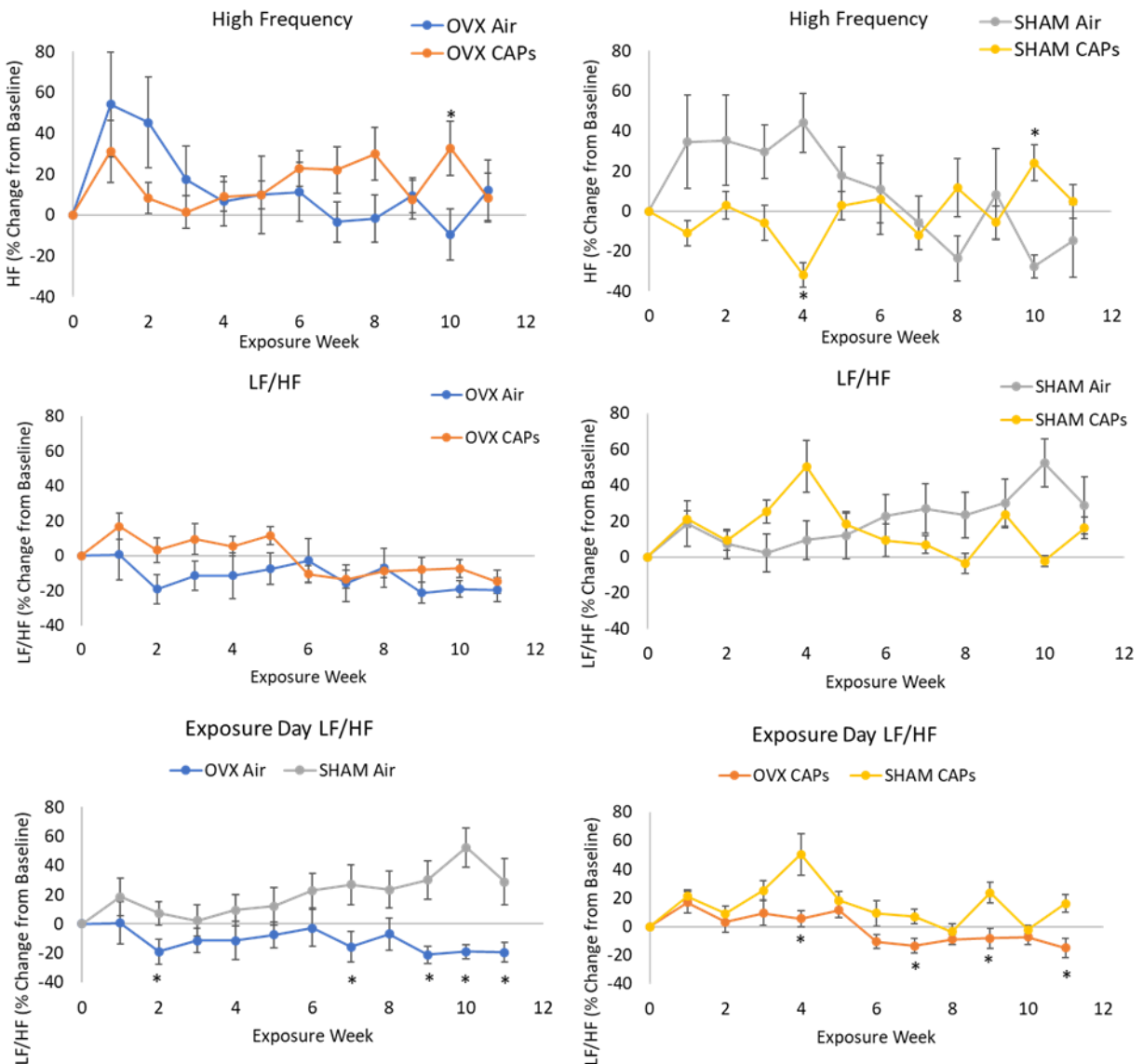


Figure 16. Frequency-domain parameters of heart rate variability (HRV).

HRV parameters were measured in the evening of each day of CAPs or Air exposure and averaged for each week for ovariectomized (OVX) and non-ovariectomized mice that underwent a sham surgery (SHAM). Note: n=4-5 per group; \*p ≤ 0.05.

### Blood Pressure

In SHAM animals, exposure to CAPs resulted in increased systolic blood pressure compared to controls, with a trend of CAPs also increasing the diastolic blood pressure (Figure 17). No effect of exposure was seen in the OVX groups.

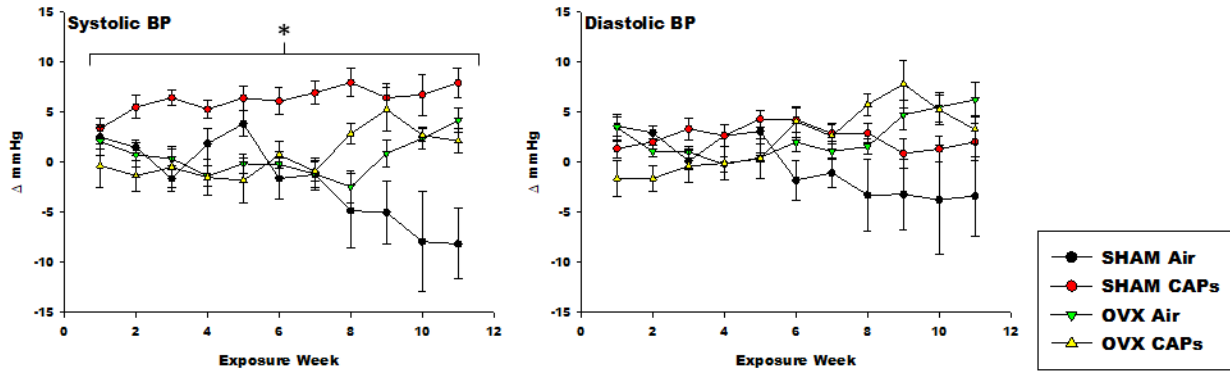


Figure 17. CAPs exposure decreased systolic blood pressure compared to controls in SHAM animals only but not in OVX mice. These plots show the change in systolic and diastolic BP ( $\Delta$  mmHg) compared to baseline (week 0) for each of the female experimental groups (Mean  $\pm$  SE; n=4-5/group). \*Sham CAPs vs. Sham Air at  $p \leq 0.05$

## Cardiac Function Measurements

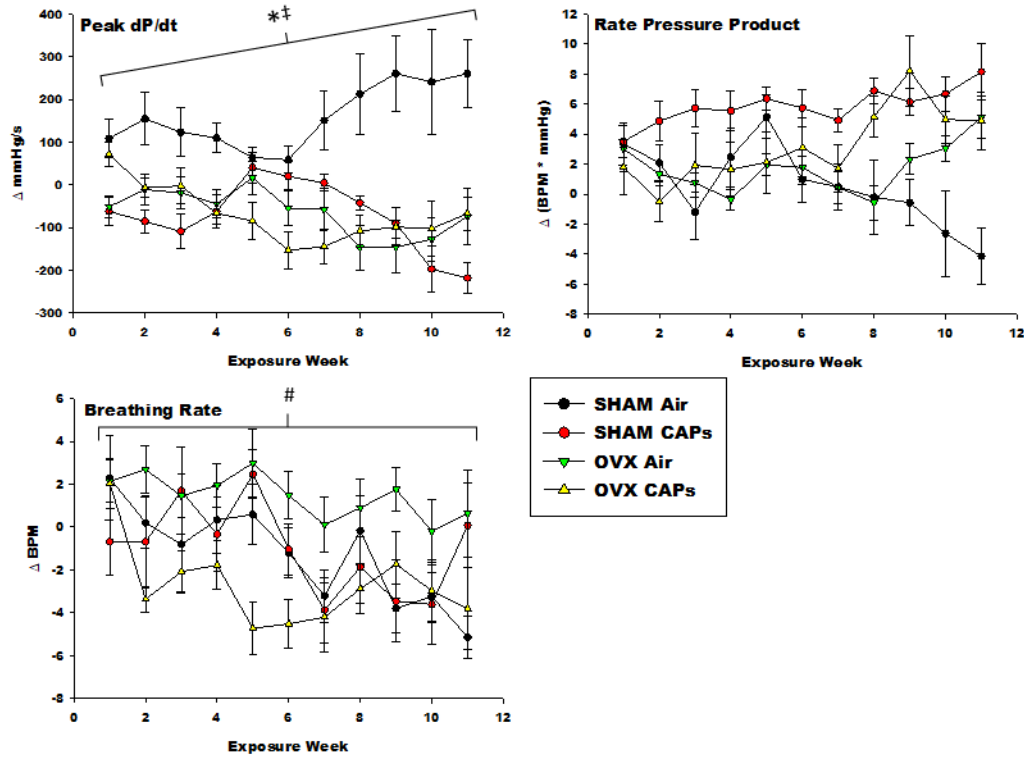


Figure 18. Exposure-related and treatment-related changes in dP/dt, rate-pressure product (RPP) and breathing rate in intact (SHAM) and OVX treated mice exposed to Air or CAPs. These plots show the change in peak dP/dt ( $\Delta$  mmHg/s), the change in Rate x Pressure, and the change in breathing rate ( $\Delta$  BPM) compared to baseline (week 0) for each of the female experimental groups (Mean  $\pm$  SE; n=4-5/group). \*Sham Air vs. OVX Air at  $P \leq 0.05$ ; #OVX CAPs vs. OVX Air at  $P \leq 0.05$ ; \*Sham CAPs vs. Sham Air at  $P \leq 0.05$

Cardiac function measurements (Figure 18) show that exposure to CAPs did not alter the rate of change in pressure measured in the aortic arch over time (dP/dt) or the rate-pressure product (RPP) in the OVX treatment, indicating left ventricular contractility and myocardial oxygen demand may not be hindered with this treatment. However, intact animals exposed to CAPs appear to exhibit decreases in both measurements compared to control animals. Lastly, the breathing rate in mice in the SHAM treatment were not affected by PM exposure while a large increase was seen in CAPs-exposed OVX animals compared to controls over the entire exposure period.

### Echocardiogram Analysis

The results shown in Figure 19 indicate that CAPs exposure caused hypertrophy (increased left ventricular (LV) mass and wall thickness) in both Sham and OVX mice, but in general effects were more pronounced in OVX mice.

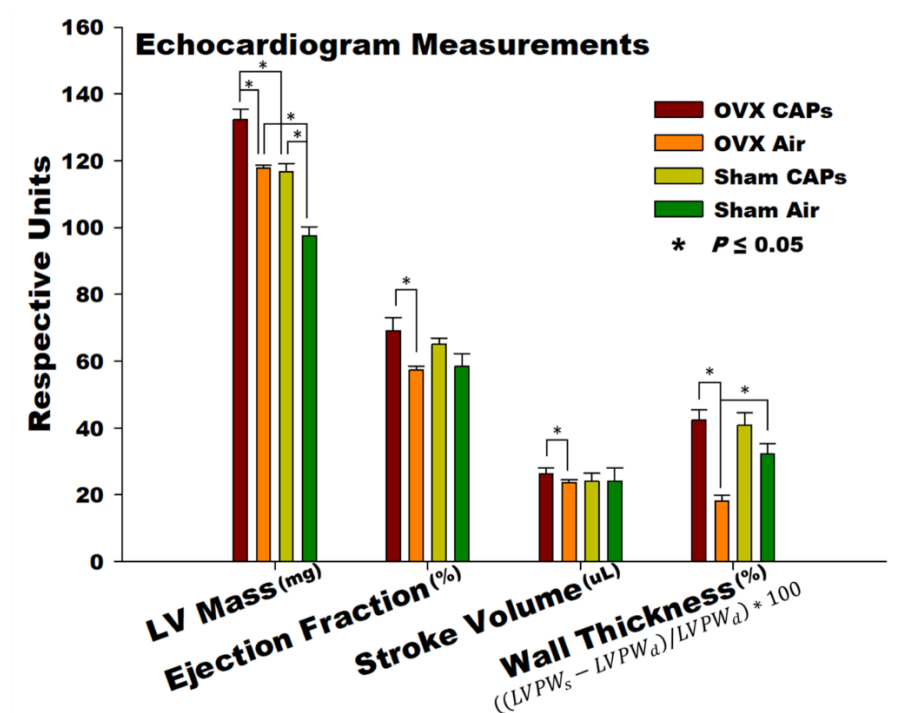


Figure 19. Echocardiogram measurements.

CAPs exposure increased left ventricular (LV) myocardial mass and wall thickness in both OVX and intact animals compared to controls, suggestive of LV hypertrophy (n = 4-5/group).

Chronic exposure to CAPs increased left ventricular (LV) myocardial mass in both OVX and intact animals compared to controls. Furthermore, the LV mass was increased in all OVX animals compared to their SHAM counterparts. Only the OVX animals exposed to PM exhibited an increased ejection fraction and stroke volume, indicating increased blood flow through the heart. Removing circulating ovarian hormones decreased LV posterior wall thickness in air exposed mice, with CAPs exposure increasing LV posterior wall thickness in only the OVX treatment.

## Cardiomyocytes

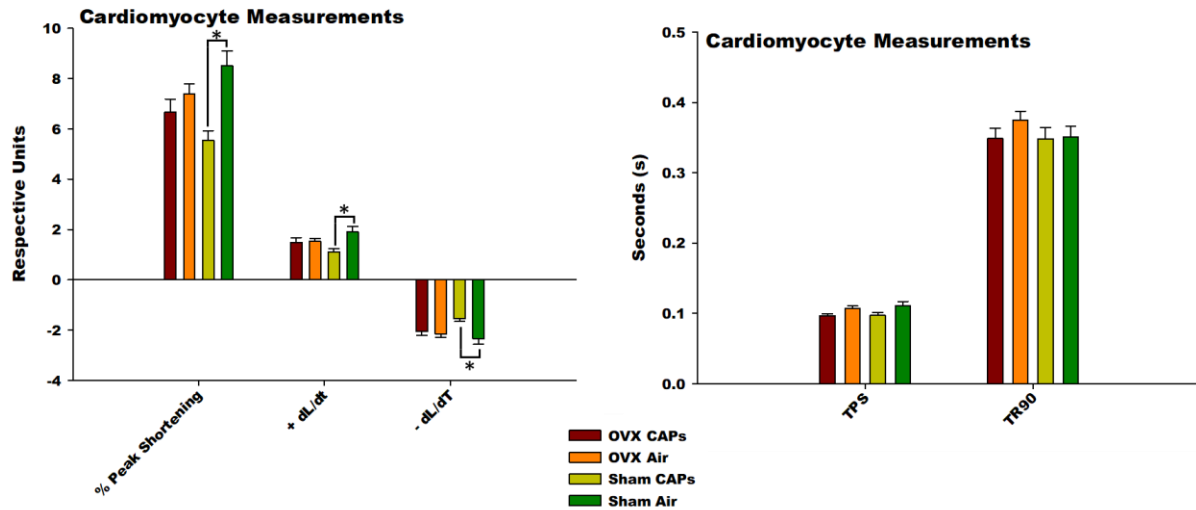


Figure 20. Cardiomyocyte contractility parameters: OVX vs. SHAM. Several contractility (shortening and lengthening) parameters were measured in cardiomyocytes from CAPs- and air-exposed females that had undergone either ovariectomy (OVX) or sham surgery (n= 4-5/group). The units of +dL/dt and -dL/dT are  $\mu\text{m}/\text{second}$ . +dL/dt = maximal velocity of relengthening; -dL/dT = maximal velocity of shortening; TPS = time to peak shortening; TR90 = time to 90% relaxation.

Cardiomyocytes were harvested and measured for various parameters of contractility. We found that the sarcomeres of intact animals exposed to CAPs exhibited decreased contractility (Figure 20) compared to controls, when looking at percent peak shortening and the maximal velocities of lengthening (+dL/dt) and shortening (-dL/dT). On the other hand, there was no effect of CAPs exposure in the OVX cohort. However, the timing of the contraction/relaxation did not differ among the four groups, as seen with the time to peak shortening (TPS) and the time to 90% relaxation (TR90). These contractility measures were similar to those identified in vivo using the invasive telemetry system.

*Plaque Formation in Arteries of Sham and OVAX Mice*

Arterial plaques from mice that had been ovariectomized (OVAX), or underwent a sham surgery, were sectioned and photographed for measurement of their total area, the area of the artery lumen, and the percent occlusion of the artery expressed as the ratio of the area of the wall to the area of the lumen. Typical sections are shown in Figure 21 with the quantification shown in Table 4. The largest and most developed plaques are seen in the SHAM-operated group exposed to CAPs. The mean plaque size was significantly greater than that of the Air-exposed SHAM ( $p \leq 0.001$ ). A two-way ANOVA showed that there was a significant effect of exposure ( $p = 0.01$ ), a significant effect of OVAX ( $p = 0.02$ ) and a significant interaction between the CAPs exposure and the OVAX surgery ( $p = 0.01$ ).

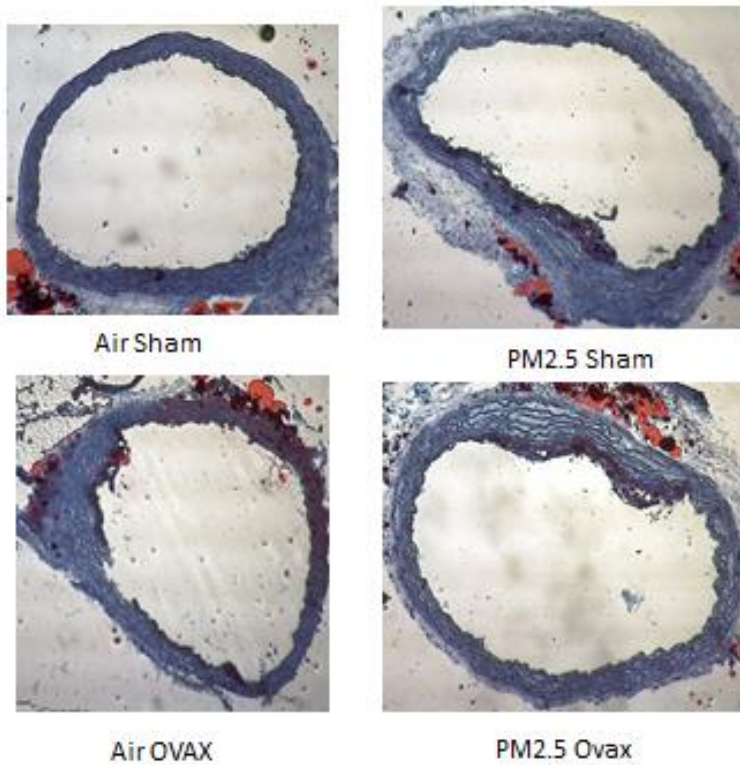


Figure 21. Arterial sections representing Air-exposed and PM<sub>2.5</sub> CAPs-exposed mice which had received sham surgeries (SHAM) or ovariectomy surgery (OVAX)

Table 4. Measurements of Arterial Plaque (n=5/group).

Area	Air Ovax	PM <sub>2.5</sub> Ovax	Air Sham	PM <sub>2.5</sub> Sham
Lumen	3.30 ± 0.41	2.90 ± 0.25	3.13 ± 0.17	2.58 ± 0.43
Wall + Plaque	2.20 ± 0.32	1.90 ± 0.19	1.98 ± 0.10	2.58 ± 0.43
Wall/Lumen Ratio	0.67 ± 0.06	0.66 ± 0.06	0.63 ± 0.03	1.08 ± 0.13

## Does 17 $\beta$ -Estradiol (E2) Rescue Adverse Cardiovascular Effects Caused by Ovariectomy and PM Exposure?

Lastly, we were interested in determining whether some of the adverse effects seen in the ovariectomized mice could be rescued with hormone replacement. Female mice underwent ovariectomy or a sham ovariectomy procedure, and half of the ovariectomized (OVAX) mice were treated with injected pellets containing a time-release dose of 17 $\beta$ -estradiol (E2) or with a placebo pellet. Two injections were required; at the beginning of the exposure study and at about week 4 of the study. In the following charts, the second injection time is noted as a vertical dashed line. Mice were exposed to CAPs or purified air (Air). Thus, there were 6 experimental groups: (1) sham surgery, air-exposed; (2) sham surgery, CAPs-exposed; (3) OVAX mice with placebo pellet, air-exposed; (4) OVAX mice with placebo pellet, CAPs-exposed; (5) OVAX mice with E2 pellet, air-exposed; and (6) OVAX mice with E2 pellet, CAPs-exposed.

The hormone-injected mice did exhibit signs of E2 toxicity (skin rashes, less activity, changes in activity) that became apparent after the second dose. The dose administered was significantly higher than the therapeutic dose and the second dose overloaded the system.<sup>1</sup> Although the hormone replacement therapy (HRT) treatment induced toxicity that became manifest 5 weeks into the exposures, the results from the first 5 weeks of study suggest that E2 treatment reduced the adverse PM-related effects noted in our first two experiments and thus provide some support for our hypothesis that ovarian toxicity, which could lead to early menopause, is an important, and previously little investigated air pollution health effect.

### *Heart Rate and Heart Rate Variability*

HRV was assessed using ecgAuto (EMKA Technologies), following the same methods for the previous studies. Due to the short battery life of the HD-X11 blood pressure transmitters, ECG data was recorded every other week to allow for complete recordings throughout the course of this study. Due to the early termination of the study, the following analyses were completed on a subset (n=3) from each group. Each data point on the following figures consists of the average of the change from baseline for the 4 exposure days of the respective exposure week.

CAPs exposure in ApoE<sup>-/-</sup> female mice had some effect on heart rate (HR) in all treatment groups (Figure 22). In ovariectomized mice with E2 hormone replacement (Ovax\_E2) as well as the placebo group (Ovax\_P) during the first few weeks of exposure, it seemed that ovariectomy, regardless of hormonal treatment, exacerbated the effect that CAPs alone had on HR. Throughout the study, HR trended towards an increase from baseline changes after CAPs exposure compared to air controls. After the second E2 pellet was administered however, the effect of CAPs exposure was eliminated, leading to both the Ovax\_E2 Air and CAPs groups to have the same increase in HR for the remainder of the study.

---

<sup>1</sup> The theoretical 17 $\beta$ -estradiol level was 8.64  $\mu$ g/mL. This is calculated from the blood volume per body weight being approximately 96 mL/kg. With a mouse having an average body weight of 20g, their blood volume would equal 1.92 mL. The two 17 $\beta$ -estradiol pellets were 1.5 mg/90 days and 1.0 mg/60 days, which is 16.6  $\mu$ g/day on average. A normal level of plasma estradiol in a mouse is several orders of magnitude lower, 56 pg/mL (Nilsson et al., Endocrinology, July 2015 Vol 156 Issue 7). Due to negative health outcomes, the study was terminated after 9 weeks.

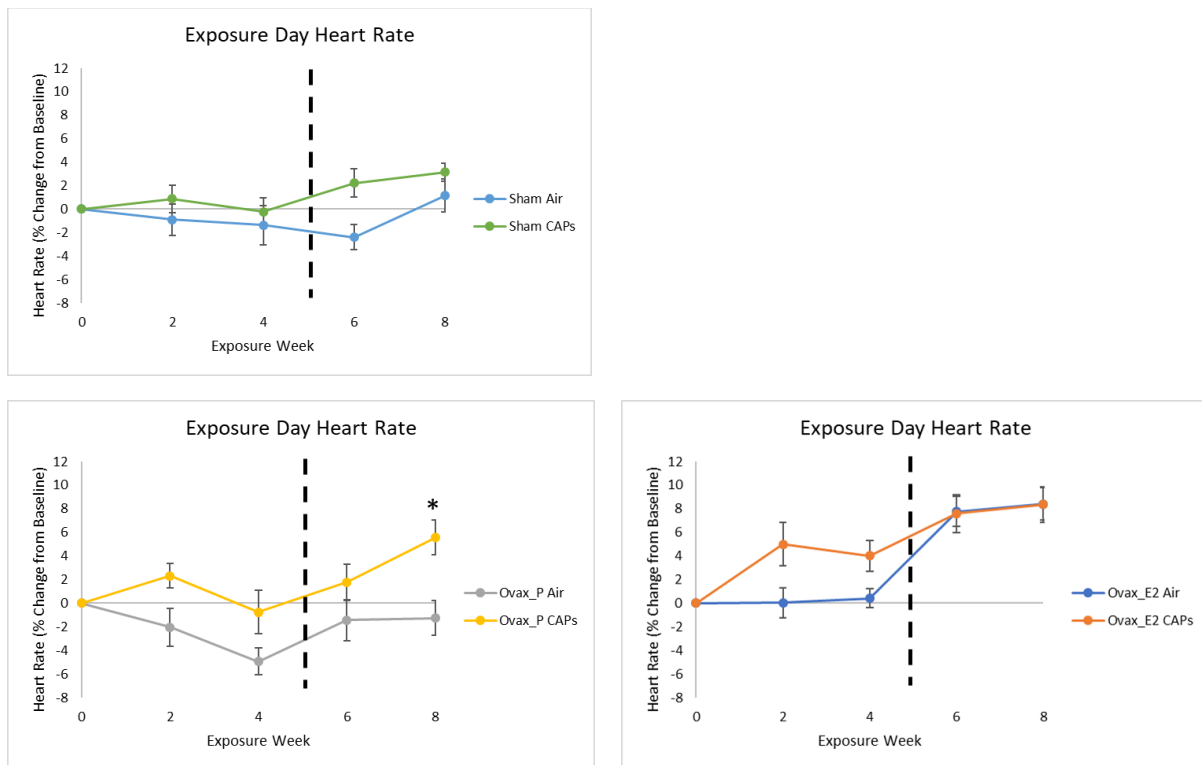


Figure 22 Heart rate changes as an effect of CAPs exposure.

Heart rates following air or CAPs exposures were compared between (top) sham groups, (bottom-left) ovariectomized mice with injected placebo pellets (Ovax\_P), and (bottom-right) ovariectomized mice with injected E2 pellets (Ovax\_E2) (Mean  $\pm$  SE; n=3/group). The vertical dashed line represents the second pellet injection of either 17 $\beta$ -estradiol or placebo at 5  $\pm$  1 weeks. \*p  $\leq$  0.05.

SDNN represents total HRV. In Figure 23, all groups exhibited a trend towards a decrease in SDNN of the CAPs-exposed animals compared to their air-exposed counterparts. This is especially seen in the latter half of the study in the ovariectomized placebo group (Ovax\_P), where the reduced HRV is significant at 6 and 8 weeks. Initially the Ovax\_E2 group followed the trend seen in Sham animals, with CAPs exposure lowering the HRV. However, after the second E2 pellet injection, the relationship changed and both Air- and CAPs-exposed animals experienced a large drop in SDNN of 20 to 30% below their baseline measures. This great reduction in HRV is associated with negative cardiovascular health.

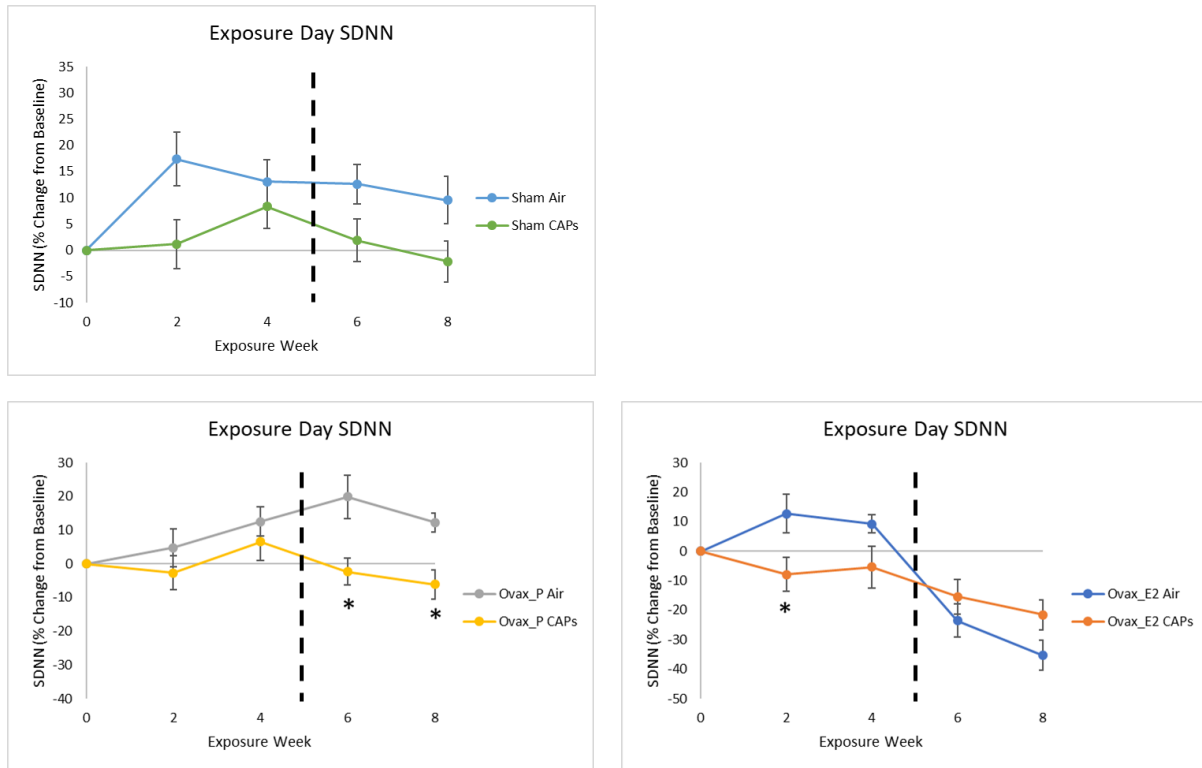


Figure 23 Total heart rate variability represented as standard deviation of NN-intervals (SDNN).

SDNN values following air or CAPs exposures were compared between (top) sham groups, (bottom-left) ovariectomized mice with injected placebo pellets (Ovax\_P), and (bottom-right) ovariectomized mice with injected E2 pellets (Ovax\_E2) (Mean  $\pm$  SE; n=3/group). The vertical dashed line represents the second pellet injection of either 17 $\beta$ -estradiol or placebo at 5  $\pm$  1 weeks. \*p  $\leq$  0.05.

RMSSD, shown in Figure 24, is interpreted as a measure of the parasympathetic nervous system input to the heart. Sham animals show an increasing separation between exposure groups over the course of the study with CAPs becoming more negative. This trend suggests, as the previous experiments have shown, that CAPs exposure is affecting the parasympathetic nervous system over time. The jagged nature of the Ovax\_E2 Air and the Ovax\_P CAPs curves is due to two individual animals which, during weeks 2 and 4 respectively, had a day of normal beats with an increase in their RMSSD. This also affected the LF/HF ratio (Figure 25) as this is another measure of the autonomic inputs.

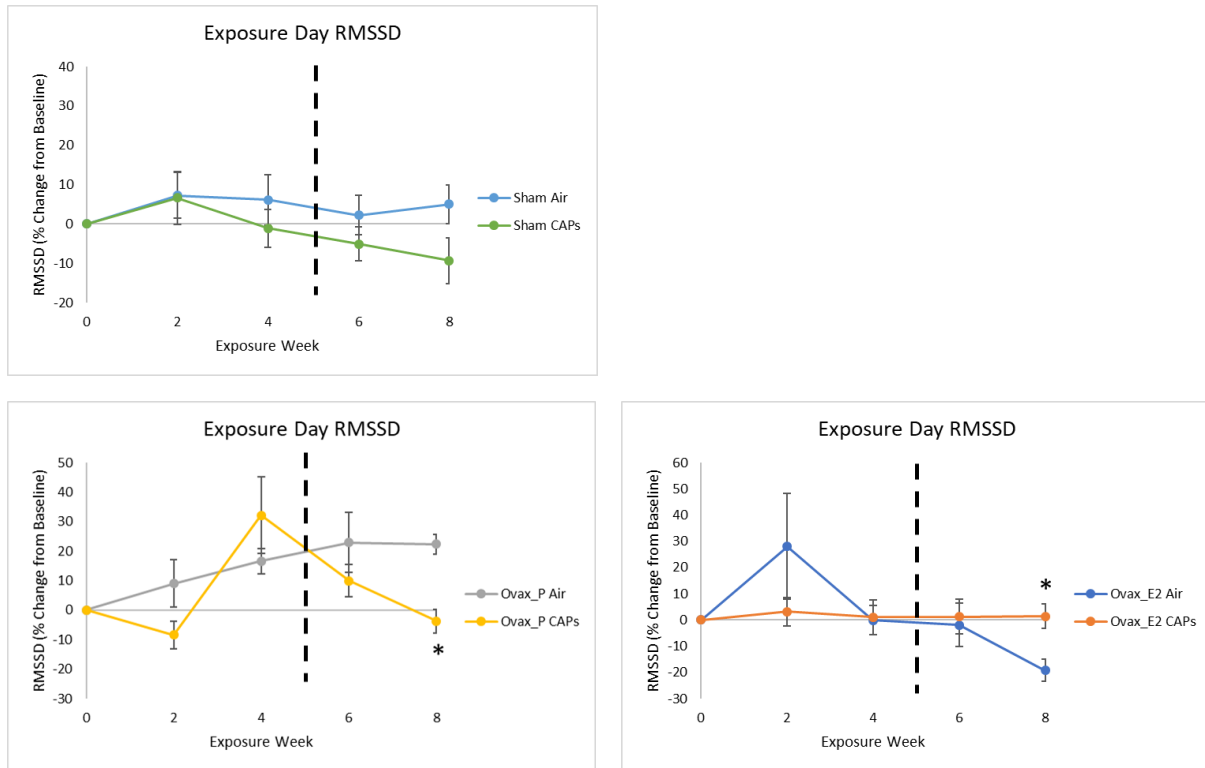


Figure 24 Root mean squared of successive differences (RMSSD) as affected by CAPs exposure and hormone treatment. RMSSD values following air or CAPs exposures were compared between (top) sham groups, (bottom-left) ovariectomized mice with injected placebo pellets (Ovax\_P), and (bottom-right) ovariectomized mice with injected E2 pellets (Ovax\_E2). (Mean  $\pm$  SE; n=3/group). The vertical dashed line represents the second pellet injection of either 17 $\beta$ -estradiol or placebo at 5  $\pm$  1 weeks. \*p  $\leq$  0.05.

The ratio of low to high frequency (LF/HF) HRV, shown in Figure 25, is theorized to represent the autonomic balance between the sympathetic and parasympathetic branches. Changes in LF/HF ratio indicate dysfunction in this important balance.

Sham animals indicate a small increase in this ratio during weeks 4 and 6 in CAPs over air, but this trend was diminished during week 8, returning to no effect of inhalation exposure. The ovariectomized groups, both E2 and P, show the greatest effect of CAPs in the final weeks of the exposure. For Ovax\_E2, the LF/HF ratio was decreased in the air exposed groups, indicating a shift to greater parasympathetic input. Responses in the Ovax\_P mice indicated there was an opposite effect of CAPs, with weeks 6 and 8 showing CAPs with a lower LF/HF ratio as compared to animals exposed to air.

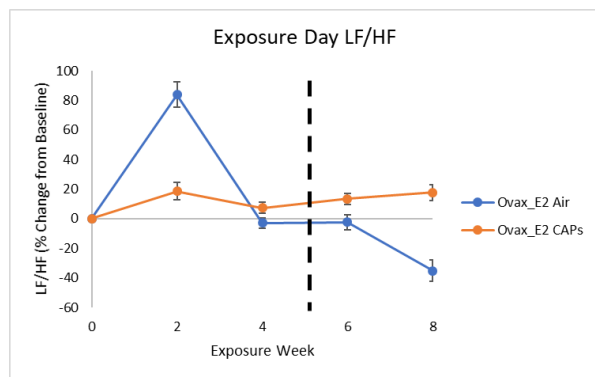
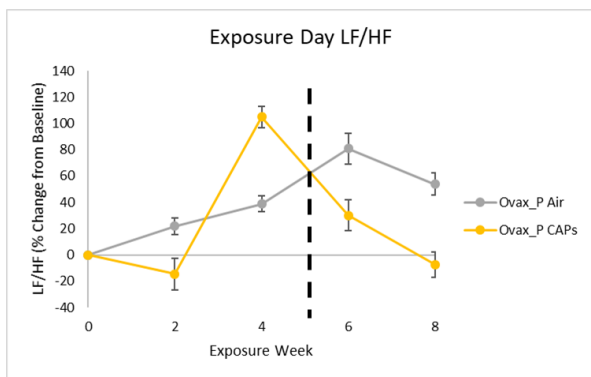
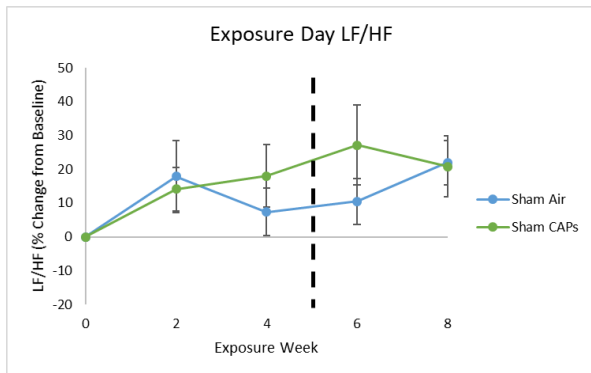


Figure 25 Ratio of low to high frequency (LF/HF) heart rate variability.

LF/HF ratios following air or CAPs exposures were compared between (top) sham groups, (bottom-left) ovariectomized mice with injected placebo pellets (Ovax\_P), and (bottom-right) ovariectomized mice with injected E2 pellets (Ovax\_E2). (Mean  $\pm$  SE; n=3/group). The vertical dashed line represents the second pellet injection of either 17 $\beta$ -estradiol or placebo at 5  $\pm$  1 weeks.

### Blood Pressure

The results of weekly non-invasive blood pressure measurements are shown in Figure 26. Because the number of animals in each group varied by week, we have summarized the n's in Table 5. In the SHAM-exposed mice, CAPs exposure increased both systolic and diastolic BP as compared with those of the air-exposed group. The CAPs-exposed OVAX/Placebo mice tended to have higher BPs than did the Air-exposed OVEX/placebo group. E2 treatment reduced BP in both Air and CAPs-exposed mice and all E2 mice had lower SBP and DBP than did the untreated mice ( $p \leq 0.05$ ). There is an obvious decreasing BP trend after the second injections around week 5, which is likely due to cumulative E2-related toxicity.

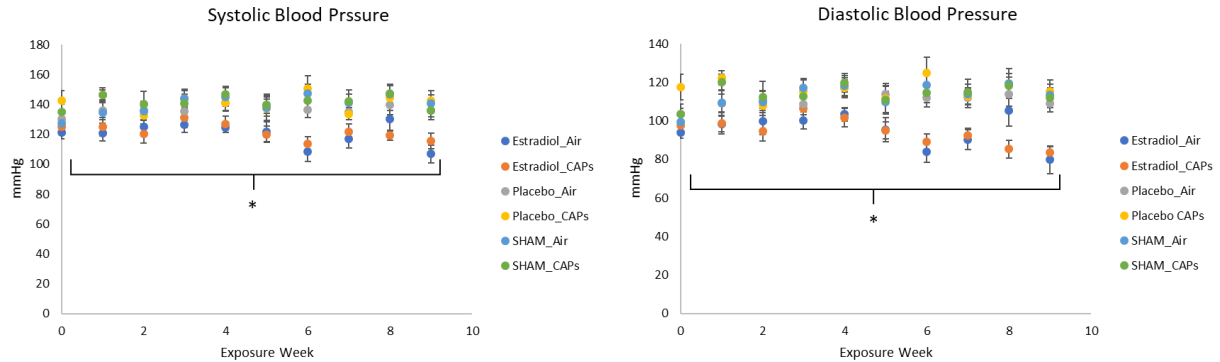


Figure 26 Systolic and diastolic blood pressure in mice exposed to Concentrated Ambient PM2.5 or purified Air. BP measures following air or CAPs exposures are plotted for the sham groups (SHAM\_Air and SHAM CAPs), the ovariectomized mice with injected placebo pellets (Placebo\_Air and Placebo\_CAPs), and the ovariectomized mice with injected E2 pellets (Estradiol\_Air and Estradiol\_CAPs) (Mean  $\pm$  SE; n varied weekly; \* E2 treatment vs. Placebo  $p < 0.05$ ).

Table 5 Number and Exposure of Mice for Blood Pressure Measurements

Date	Week	E2	P	S	E2	E2	P	P	S	S
Group/Exposure		Total			Air	CAPs	Air	CAPs	Air	CAPs
9/2/2019	0	22	24	28	12	10	12	12	16	12
9/9/2019	1	20	22	22	11	9	11	11	12	10
9/16/2019	2	22	24	28	12	10	12	12	16	12
9/23/2019	3	22	23	28	12	10	12	11	16	12
9/30/2019	4	20	23	27	10	10	12	11	16	11
10/7/2019	5	20	23	27	10	10	12	11	16	11
10/14/2019	6	19	23	27	9	10	12	11	16	11
10/21/2019	7	19	22	26	9	10	12	10	15	11
10/28/2019	8	18	22	26	8	10	12	10	15	11
11/4/2019	9	15	23	27	7	8	12	11	16	11

E2 = 17 $\beta$ -estradiol treatment, P = placebo treatment, S = SHAM surgery

## Limitations of this study

The goal of this study was to examine the effects of PM exposure on female health. While there is strong epidemiological evidence that post-menopausal women are at elevated risk for cardiovascular and heart disease and that cardiovascular and heart disease morbidity and mortality are strongly associated with exposure to PM<sub>2.5</sub>, this study is the first to examine links between adverse female cardiac outcomes and PM<sub>2.5</sub> exposure under controlled conditions. An obvious limitation of this study is that the subjects were mice and that the mice were genetically modified to increase their susceptibility to developing arterial plaques (similar to plaques that form in humans with elevated LDL-cholesterol levels). However, to the extent possible we performed the study under controlled conditions and used appropriate experimental controls, controlled the animal's diet and purified the air the animals breathed when they were not being specifically exposed to pollutants. The daily exposure concentrations were higher than the 24 hr ambient air quality standard, but the exposures were 5 hr per day for 4 days per week. If we convert that to a 'human equivalent' exposure, where humans are exposed 24 hr per day, 7 days per week, our exposures would be below the ambient air standard. In fact, our exposures are not significantly different from peak ambient exposure levels reported for California cities (even on days without inundation with forest fire smoke). Mouse cardiac physiology is similar to, but not identical with, human cardiac physiology. For example, there are interspecies differences in ECG waveforms, which we take into account to the best of our ability when interpreting our physiology results. The cumulative HRT dose we used was too high and as the time-release E2 hormone built up in the mice we reached a dose when there was frank toxicity, so we consider data after the 5<sup>th</sup> week of exposures to be unreliable. We can't rule out E2 effects even at the earlier times, however, we did have results from our placebo controls and there was good agreement between the Air-E2 and the Air-placebo, for example for heart rate variability (HRV) which provides some support that the PM-induced reduction in HRV was partially offset by the E2 replacement. We observed potentially beneficial effects of HRT, albeit at near-toxic levels. Future experiments should be performed at lower doses and a range of doses should be tested to determine the potentially therapeutic dose range before attempting longer term studies.

## Summary and Conclusions

The primary hypothesis tested in this long-term exposure study was that there were differences in the response of males and females exposed to CAPs. As shown in Table 6, the largest and most significant cumulative changes in electrocardiography, heart rate variability, hemodynamics and cardiopulmonary function occurred in females. These changes were possibly coincident, and consistent with, the loss of primary and secondary ovarian follicles, as determined at the end of the 12-week exposures.

*Table 6 Summary of Responses in Male and Female apoE<sup>-/-</sup> Mice Exposed to CAPs.*

		Predominant Direction of Change During 12 weeks of Exposure	
		Male	Female
		CAPs vs Air	CAPs vs Air
Electrocardiography	HR	↓	↓
	P wave	NC	↑
	PR int	↑*	↓
	QRS int	↓*	↑
	QT interval	↓	↓
Heart Rate Variability	HR	NC	
	SDNN	↓	↓**
	RMSSD	↓	↓**
Blood Pressure	Systolic	↓	↑*
	Diastolic	↓	↑*
Cardiopulmonary Function	dp/dt	NC	
	RPP	↓	↑
	Breath Rate	NC	↓*
Effects on Ovarian Follicles in Exposed Female Mice	Primordial	NA	↓
	Primary	NA	↓*
	Healthy 2 <sup>o</sup>	NA	↓*
	Atretic 2 <sup>o</sup>	NA	NS
	Antral	NA	NS
*p ≤ 0.05; ** p ≤ 0.01; NC = No Consistent Change; NA = Not Applicable			

HRV measures after exposure to PM<sub>2.5</sub> CAPs showed a general decreasing trend. Decreases in RMSSD in both males and females reflect changes to parasympathetic nervous system inputs to the heart after chronic air pollution exposure. HR and HRV measures changed drastically from the initial few weeks of exposure to the end of the 11 weeks, demonstrating the need for chronic exposure studies to more fully understand the potential for negative health outcomes. Sex-differences are evident in CAPs-induced HRV changes, with females showing a greater negative HRV response to CAPs exposure than did males,

highlighting sex-differences in cardiovascular effects of PM inhalation. Changes in autonomic nervous system control of heart rate are considered a biomarker for stress in general, and in individuals with cardiovascular disease, decreased HRV is considered to be an adverse outcome (Fakhri et al. 2009; Guan et al. 2018; Jarczok et al. 2014; Magari et al. 2002).

In highlighting other key sex differences, male animals appeared to be more susceptible to atrial conduction anomalies as indicated by large P-R interval elongation compared to air controls, which was not seen in the females. Chronic exposure to CAPs also produced marked changes in ventricular conduction rates. Exposed male mice experienced shorter ventricular depolarization/repolarization cycles compared to air controls while no exposure effect was seen in the female animals.

While there have been many studies demonstrating that there are interactions between ovarian and cardiovascular function, the modulatory role of perturbations in ovarian function on the cardiovascular effects of exposure to PM had not been investigated until now. In this project, we showed that air pollution exposure indeed had a direct effect on the ovaries. Exposure to PM<sub>2.5</sub> CAPs for 5 hours/day, 4 days/week, for 12 weeks decreased ovarian primary and primordial follicle numbers, resulting in about a 50% depletion of the ovarian reserve. Numbers of growing secondary follicles were also decreased. Follicle depletion was not associated with accelerated recruitment of primordial follicles into the growing pool or with increased activation of caspase 3 in the follicles at any stage of development. Decreased ovarian reserve leads to premature ovarian failure, which increases the risk for cardiovascular disease in women. Thus, our data support the hypothesis that exposure to PM<sub>2.5</sub> may increase the risk for cardiovascular disease in women by accelerating the onset of ovarian senescence.

We examined the development of plaque in the arteries of intact (SHAM) and ovariectomized (OVAX) mice exposed to Air or CAPs. The largest and most developed plaques were seen in the SHAM group exposed to CAPs. The mean plaque size was significantly greater than that of the Air-exposed SHAM group ( $p \leq 0.001$ ). A two-way ANOVA showed that there was a significant effect of exposure ( $p = 0.01$ ), a significant effect of OVAX ( $p = 0.02$ ) and a significant interaction between the CAPs exposure and the OVAX surgery ( $p = 0.01$ ). CAPs exposure increased LV myocardial mass and wall thickness in both OVX and intact animals compared to control female mice. The induction of LV hypertrophy by PM<sub>2.5</sub> CAPs exposure has not been previously demonstrated under controlled conditions, to our knowledge, although there is epidemiological evidence that LV function is sub-clinically impaired in individuals chronically exposed to ambient PM<sub>2.5</sub>. The implication of LV dysfunction being induced by PM<sub>2.5</sub> exposures in an animal model that recapitulates some aspects of post-menopause may suggest a link between air pollution exposure and increased risk of heart disease in women, which is especially significant since our findings indicate that, compared to Air exposure in intact mice, PM<sub>2.5</sub> exposure induced larger plaques and reduced numbers of primordial, primary ( $p \leq 0.05$ ) and healthy secondary ( $p \leq 0.05$ ) ovarian follicles which would likely accelerate ovarian 'aging'. Overall our findings suggest an association between PM effects on ovarian function and PM effects on arterial plaque formation and are consistent with epidemiological findings of increased risk of cardiovascular disease in post-menopausal women.

E2 treatment reduced BP in both Air and CAPs-exposed mice and all E2 mice had lower SBP and DBP than did the untreated mice. Overall, our interim analyses indicate that CAPs does affect HR and HRV measures, in both the time and frequency domains and that ovariectomy augments the CAPs effects. Sham animals show trends of a decrease in overall HRV, as well as a shift of decreasing parasympathetic

input to the heart with exposure to CAPs. Animals with ovariectomies and a placebo hormone replacement follow overall similar trends of the effect of CAPs as seen in the Sham animals in all measures however slightly more pronounced. The addition of the E2 hormone replacement in Ovax\_E2 groups have two phases of their HRV affects: before and after the second E2 pellet injection. The second pellet injection created a directional switch in the relationship of Air and CAPs exposure effects, as well as created an overall decrease in all HRV measures. Despite the likely toxic levels of E2, the present study shows evidence of a palliative effect of hormone replacement after ovariectomy on the heart and autonomic function in PM-exposed mice.

While we have gained valuable insight from our work, further research is needed to continue to elucidate the mechanisms of why older females are more susceptible to adverse health effects from air pollution. In addition, there are other aspects of reproductive health that need to be investigated. For example, extrapolating the effects seen in this study to longer exposure durations would predict increased infertility and possibly sub-lethal damage to ovarian cells that could have implications for the health of offspring of still-fertile dams, which might be consistent with epidemiological findings of decreased infant birth weights and toxicological findings that effects of PAH exposures could have transgenerational effects. Next steps in this research would be to examine factors such as time to menopause (our study suggests that might be shortened), changes in fertility and health of the offspring after in utero exposures and whether changes in male germ cells (suggested by some of our preliminary data) might impact fertility and developmental toxicity.

## References

- Araujo JA, Barajas B, Kleinman M, Wang X, Bennett BJ, Gong KW, et al. 2008. Ambient particulate pollutants in the ultrafine range promote early atherosclerosis and systemic oxidative stress. *Circ Res* 102:589-596.
- Boukens BJ, Rivaud MR, Rentschler S, Coronel R. 2014. Misinterpretation of the mouse ecg: 'Musing the waves of mus musculus'. *The Journal of Physiology* 592:4613-4626.
- Bourassa P-AK, Milos PM, Gaynor BJ, Breslow JL, Aiello RJ. 1996. Estrogen reduces atherosclerotic lesion development in apolipoprotein e-deficient mice. *Proc Natl Acad Sci U S A* 93:10022-10027.
- Charleston JS, Hansen KR, Thyer AC, Charleston LB, Gougeon A, Siebert JR, et al. 2007. Estimating human ovarian non-growing follicle number: The application of modern stereology techniques to an old problem. *Hum Reprod* 22:2103-2110.
- de Gooyer TE, Skinner SL, Wlodek ME, Kelly DJ, Wilkinson-Berka JL. 2004. Angiotensin ii influences ovarian follicle development in the transgenic (mren-2)27 and sprague dawley rat. *J Endocrinol* 180:311-324.
- Dubey RK, Imthurn B, Barton M, Jackson EK. 2005. Vascular consequences of menopause and hormone therapy: Importance of timing of treatment and type of estrogen. *Cardiovasc Res* 66:295-306.
- Farraj AK, Hazari MS, Haykal-Coates N, Lamb C, Winsett DW, Ge Y, et al. 2011. St depression, arrhythmia, vagal dominance, and reduced cardiac micro-rna in particulate-exposed rats. *Am J Respir Cell Mol Biol* 44:185-196.
- Fleisher LA, Frank SM, Sessler DI, Cheng C, Matsukawa T, Vannier CA. 1996. Thermoregulation and heart rate variability. *Clin Sci (Lond)* 90:97-103.
- Goldbarg AN, Hellerstein HK, Bruell JH, Daroczy AF. 1968. Electrocardiogram of the normal mouse, mus musculus: General considerations and genetic aspects. *Cardiovasc Res* 2:93-99.
- Gottipolu RR, Wallenborn JG, Karoly ED, Schladweiler MC, Ledbetter AD, Krantz T, et al. 2009. One-month diesel exhaust inhalation produces hypertensive gene expression pattern in healthy rats. *Environ Health Perspect* 117:38-46.
- Hayano J, Yamada A, Mukai S, Sakakibara Y, Yamada M, Ohte N, et al. 1991. Severity of coronary atherosclerosis correlates with the respiratory component of heart rate variability. *Am Heart J* 121:1070-1079.
- Kamdar O, Le WW, Zhang J, Ghio AJ, Rosen GD, Upadhyay D. 2008. Air pollution induces enhanced mitochondrial oxidative stress in cystic fibrosis airway epithelium. *FEBS Lett* 582:3601-3606.
- Kaplan JR, Adams MR, Clarkson TB, Manuck SB, Shively CA, Williams JK. 1996. Psychosocial factors, sex differences, and atherosclerosis: Lessons from animal models. *Psychosom Med* 58:598-611.
- Kim S, Jaques PA, Chang M, Barone T, Xiong C, Friedlander SK, et al. 2001. Versatile aerosol concentration enrichment system (vaces) for simultaneous in vivo and in vitro evaluation of toxic effects of ultrafine, fine and coarse ambient particles part ii: Field evaluation. *Journal of Aerosol Science* 32:1299-1314.
- Kim S, Jaques PA, Chang MC, Barone T, Xiong C, Friedlander SK, et al. 2001a. Versatile aerosol concentration enrichment system (vaces) for simultaneous in vivo and in vitro evaluation of toxic effects of ultrafine, fine and coarse ambient particles - part ii: Field evaluation. *J Aerosol Sci* 32:1299-1314.

- Kim S, Jaques PA, Chang MC, Froines JR, Sioutas C. 2001b. Versatile aerosol concentration enrichment system (vaces) for simultaneous in vivo and in vitro evaluation of toxic effects of ultrafine, fine and coarse ambient particles - part i: Development and laboratory characterization. *J Aerosol Sci* 32:1281-1297.
- Kleinman MT, Sioutas C, Froines JR, Fanning E, Hamade A, Mendez L, et al. 2007. Inhalation of concentrated ambient particulate matter near a heavily trafficked road stimulates antigen-induced airway responses in mice. *Inhalation Toxicology* 19 Suppl 1:117-126.
- Lewtas J. 2007. Air pollution combustion emissions: Characterization of causative agents and mechanisms associated with cancer, reproductive, and cardiovascular effects. *Mutat Res* 636:95-133.
- Li Z, Hyseni X, Carter JD, Soukup JM, Dailey LA, Huang Y-CT. 2006. Pollutant particles enhanced  $\text{h}_2\text{O}_2$  production from nad(p)h oxidase and mitochondria in human pulmonary artery endothelial cells. *Am J Physiol* 291:C357-C365.
- Liao D, Cai J, Barnes RW, Tyroler HA, Rautaharju P, Holme I, et al. 1996. Association of cardiac autonomic function and the development of hypertension: The aric study. *Am J Hypertens* 9:1147-1156.
- Lopez SG, Luderer U. 2004. Effects of cyclophosphamide and buthionine sulfoximine on ovarian glutathione and apoptosis. *Free Radic Biol Med* 36:1366-1377.
- Lossius K, Eriksen M, Walløe L. Thermoregulatory fluctuations in heart rate and blood pressure in humans: Effect of cooling and parasympathetic blockade. *Journal of the Autonomic Nervous System* 47:245-254.
- Mayer LP, Dyer CA, Eastgard RL, Hoyer PB, Banka CL. 2005. Atherosclerotic lesion development in a novel ovary-intact mouse model of perimenopause. *Arterioscler Thromb Vasc Biol* 25:1910-1916.
- Miller KA, Siscovick DS, Sheppard L, Shepherd K, Sullivan JH, Anderson GL, et al. 2007. Long-term exposure to air pollution and incidence of cardiovascular events in women. *N Engl J Med* 356:447-458.
- Mitchell GF, Jeron A, Koren G. 1998. Measurement of heart rate and q-t interval in the conscious mouse. *Am J Physiol* 274:H747-751.
- Mohallem SV, de Araújo Lobo DJ, Pesquero CR, Assunção JV, de Andre PA, Saldivo PHN, et al. 2005. Decreased fertility in mice exposed to environmental air pollution in the city of sao paulo. *Environ Res* 98:196-202.
- Monreal G, Nicholson LM, Han B, Joshi MS, Phillips AB, Wold LE, et al. 2008. Cytoskeletal remodeling of desmin is a more accurate measure of cardiac dysfunction than fibrosis or myocyte hypertrophy. *Life Sci* 83:786-794.
- Myers M, Britt KL, Wreford NGM, Ebling FJP, Kerr JB. 2004. Methods for quantifying follicular numbers within the mouse ovary. *Reproduction* 127:569-580.
- Norby FL, Wold LE, Duan J, Hintz KK, Ren J. 2002. Igf-i attenuates diabetes-induced cardiac contractile dysfunction in ventricular myocytes. *Am J Physiol Endocrinol Metab* 283:E658-666.
- Oldham MJ, Phalen RF, Robinson RJ, Kleinman MT. 2004. Performance of a portable whole-body mouse exposure system. *Inhalation Toxicology* 16:657-662.

- Pinilla L, Castellano JM, Romero M, Tena-Sempere M, Gaytán F, Aguilar E. 2009. Delayed puberty in spontaneously hypertensive rats involves a primary ovarian failure independent of the hypothalamic kiss-1/gpr54/gnrh system. *Endocrinology* 150:2889-2897.
- Plowchalk DR, Smith BJ, Mattison DR. 1993. Assessment of toxicity to the ovary using follicle quantitation and morphometrics. In: *Female reproductive toxicology*, Vol. 3B, (Heindel JJ, Chapin RE, eds). San Diego, CA:Academic Press, 57-68.
- Pope CAI, Burnett RT, Thurston GD, Thun MJ, Calle EE, Krewski D, et al. 2004. Cardiovascular mortality and long-term exposure to particulate air pollution: Epidemiological evidence of general pathophysiological pathways of disease. *Circulation* 109:71-77.
- Rubes J, Selevan SG, Evenson DP, Zudova D, Vozdova M, Zudova Z, et al. 2005. Episodic air pollution is associated with increased DNA fragmentation in human sperm without other changes in semen quality. *Hum Reprod* 20:2276-2283.
- Rubes J, Selevan SG, Sram RJ, Evenson DP, Perreault SD. 2007. Gstm1 genotype influences the susceptibility of men to sperm DNA damage associated with exposure to air pollution. *Mutat Res* 625:20-28.
- Selevan SG, Borkovec L, Slott VL, Zudová Z, Rubeš J, Evenson DP, et al. 2000. Semen quality and reproductive health of young czech men exposed to seasonal air pollution. *Environ Health Perspect* 108:887-894.
- Shuster LT, Gostout BS, Grossardt BR, Rocca WA. 2008. Prophylactic oophorectomy in premenopausal women and long-term health. *Menopause Int* 14:111-116.
- Souza VR, Mendes E, Casaro M, Antiorio A, Oliveira FA, Ferreira CM. 2019. Description of ovariectomy protocol in mice. *Methods Mol Biol* 1916:303-309.
- Speerschneider T, Thomsen MB. 2013. Physiology and analysis of the electrocardiographic t wave in mice. *Acta Physiol (Oxf)* 209:262-271.
- Storment JM, Meyer M, Osol G. 2000. Estrogen augments the vasodilatory effects of vascular endothelial growth factor in the uterine circulation of the rat. *Am J Obstet Gynecol* 183:449-453.
- Strehlow K, Rotter S, Wassmann S, Adam O, Grohé C, Laufs K, et al. 2003. Modulation of antioxidant enzyme expression and function by estrogen. *Circ Res* 93:170-177.
- Sun Q, Yue P, Deiuliis JA, Lumeng CN, Kampfrath T, Mikolaj MB, et al. 2009. Ambient air pollution exaggerates adipose inflammation and insulin resistance in a mouse model of diet-induced obesity. *Circulation* 119:538-546.
- Upadhyay D, Panduri V, Ghio A, Kamp DW. 2003. Particulate matter induces alveolar epithelial cell DNA damage and apoptosis. *Am J Respir Cell Mol Biol* 29:180-187.
- Veras MM, Damaceno-Rodrigues NR, Guimarães Silva RM, Scoriza JN, Nascimento Saldiva PH, Garcia Caldini E, et al. 2009. Chronic exposure to fine particulate matter emitted by traffic affects reproductive and fetal outcomes in mice. *Environ Res* 109:536-543.
- Wassmann S, Bäumer AT, Strehlow K, van Eickels M, Grohé C, Ahlbory K, et al. 2001. Endothelial dysfunction and oxidative stress during estrogen deficiency in spontaneously hypertensive rats. *Circulation* 103:435-441.

- Whaley-Connell A, Habibi J, Cooper SA, DeMarco VG, Hayden MR, Stump CS, et al. 2008. Effect of renin inhibition and at<sub>1</sub>r blockade on myocardial remodeling in the transgenic ren2 rat. *Am J Physiol* 295:E103-E109.
- Wold LE, Relling DP, Duan J, Norby FL, Ren J. 2002. Abrogated leptin-induced cardiac contractile response in ventricular myocytes under spontaneous hypertension: Role of jak/stat pathway. *Hypertension* 39:69-74.
- Wold LE, Muralikrishnan D, Albano CB, Norby FL, Ebadi M, Ren J. 2003. Insulin-like growth factor i (igf-1) supplementation prevents diabetes-induced alterations in coenzymes q9 and q10. *Acta Diabetol* 40:85-90.
- Wold LE, Ying Z, Hutchinson KR, Velten M, Gorr MW, Velten C, et al. 2012. Cardiovascular remodeling in response to long-term exposure to fine particulate matter air pollution. *Circ Heart Fail* 5:452-461.
- Xia T, Korge P, Weiss JN, Li N, Venkatesen MI, Sioutas C, et al. 2004. Quinones and aromatic chemical compounds in particulate matter induce mitochondrial dysfunction: Implications for ultrafine particle toxicity. *Environ Health Perspect* 112:1347-1358.
- Xia T, Kovochich M, Nel AE. 2007. Impairment of mitochondrial function by particulate matter (pm) and their toxic components: Implications for pm-induced cardiovascular disease and lung disease. *Front Biosci* 12:1238-1246.
- Yang Z, Harrison CM, Chuang GC, Ballinger SW. 2007. The role of tobacco smoke induced mitochondrial damage in vascular dysfunction and atherosclerosis. *Mutat Res* 621:61-74.